

## Article

# Characteristic Analysis of Carbon Sink Capacity Changes in Xinjiang's Terrestrial Ecosystem Based on EEMD

Yongji Zhang <sup>1</sup>, Jianghua Zheng <sup>1,2,\*</sup>, Jianli Zhang <sup>3</sup>, Chen Mu <sup>3</sup>, Wanqiang Han <sup>1</sup> and Liang Liu <sup>1</sup><sup>1</sup> College of Geography and Remote Sensing Sciences, Xinjiang University, Urumqi 830046, China<sup>2</sup> Xinjiang Key Laboratory of Oasis Ecology, Xinjiang University, Urumqi 830046, China<sup>3</sup> Prairie Station of Animal Husbandry Department in Xinjiang, Urumqi 830000, China

\* Correspondence: zheng.jianghua@xju.edu.cn

**Abstract:** Net Ecosystem Productivity (NEP) is an important measure to assess the carbon balance and dynamics of ecosystems, providing a direct measure of carbon source–sink dynamics in terrestrial ecosystems and finding widespread applications in carbon cycle research. However, the nonlinear characteristics of NEP in Xinjiang's terrestrial ecosystems remain unclear. Additionally, the influence of land use patterns, temperature, and precipitation variations on carbon sink capacity remains unclear. Ensemble Empirical Mode Decomposition (EEMD) is used to investigate the nonlinear variation of NEP in Xinjiang. Landscape pattern analysis of Xinjiang's land use patterns from 1981 to 2019 is conducted using a 30 km moving window, and the interannual relationships between NEP, land use patterns, and meteorological factors are investigated through EEMD detrending analysis and Pearson correlation. The findings indicate that: (1) NEP exhibits interannual variations, primarily concentrated in the foothills of the Tianshan Mountains, with a three-year cycle. (2) Although NEP changes in most regions are not significant, urban clusters on the northern slopes of the Tianshan Mountains show noteworthy trends, with initial decrease followed by an increase, covering around 34.87% of the total area. Areas at risk of NEP decline constitute approximately 7.32% of the total area. (3) Across Xinjiang, we observe a widespread rise in patch fragmentation and complexity, coupled with a decline in patch connectivity and the size of the dominant patch. Additionally, there is a notable increase in both the diversity and evenness of land use types. However, the correlation between land use patterns and NEP is generally found to be insignificant in the majority of areas, with a percentage exceeding 85%. (4) Approximately 62% of regions in Xinjiang have NEP that is positively correlated with temperature, with significance observed in 33% of these areas. Furthermore, almost 95% of regions demonstrate that NEP is positively correlated with precipitation, with significance noted in 83% of these regions. It appears that precipitation exerts a more pronounced influence on NEP fluctuations in Xinjiang when compared to temperature.

**Keywords:** net ecosystem productivity (NEP); nonlinear characteristics; ensemble empirical modal decomposition (EEMD); carbon source/sink; land use patterns



**Citation:** Zhang, Y.; Zheng, J.; Zhang, J.; Mu, C.; Han, W.; Liu, L. Characteristic Analysis of Carbon Sink Capacity Changes in Xinjiang's Terrestrial Ecosystem Based on EEMD. *Sustainability* **2024**, *16*, 2277. <https://doi.org/10.3390/su16062277>

Academic Editors: Baojie He, Siliang Yang, K. Venkatachalam and Amos Darko

Received: 3 February 2024

Revised: 3 March 2024

Accepted: 7 March 2024

Published: 8 March 2024



**Copyright:** © 2024 by the authors. Licensee MDPI, Basel, Switzerland. This article is an open access article distributed under the terms and conditions of the Creative Commons Attribution (CC BY) license (<https://creativecommons.org/licenses/by/4.0/>).

## 1. Introduction

Global terrestrial ecosystems are indispensable to the carbon cycle [1]. As a vast carbon reservoir, terrestrial vegetation absorbs a substantial amount of carbon dioxide through photosynthesis, storing it in plant tissues. Concurrently, soil acts as a substantial reservoir for organic carbon that is capable of counterbalancing more than 30% of yearly anthropogenic carbon emissions [2]. NEP quantifies the net carbon exchange between terrestrial ecosystems and the atmosphere, indicating the balance between carbon sources and sinks. It is determined by subtracting soil heterotrophic respiration from the net carbon fixed by terrestrial ecosystems. This metric illustrates the pace of variation in net carbon flux or carbon stocks between the land and the atmosphere [3]. NEP serves as a direct indicator of the carbon source or sink status within terrestrial ecosystems [4]. Therefore,

monitoring changes in NEP is instrumental for ecosystem management and conservation efforts, furnishing a scientific groundwork for crafting adaptive policies to tackle global transformations [5].

NEP is influenced by a variety of environmental factors, including CO<sub>2</sub> levels in the atmosphere and climatic conditions. Besides these, alterations in land use patterns, such as ecological restoration, agricultural practices, and urban development, can significantly impact carbon sequestration rates and storage, thus altering the carbon balance in terrestrial ecosystems [6]. Land Use and Land Cover Change (LUCC) are the primary expressions of human activities interacting with the natural environment. It directly alters ecosystem types, structures, and functions, subsequently affecting the NEP of ecosystems [7]. Previous studies have thoroughly examined the effects of land use change on NEP. Xu et al. used the enhanced BIOME-BGC model to assess the impact of Taihu Lake Basin land use change on the NEP between 1985 and 2010 [8]. Similarly, Gao et al. estimated the impact of land use and LUCC on the NEP in the 1980–1990's in the intercrossing zone of China [9]. Monitoring changes in landscape patterns can offer detailed insights into the dynamics of land use changes, thus enhancing our understanding of the long-term effects of these changes on the patterns of carbon sinks [10]. However, existing research has predominantly focused on data analysis for the initial and final years of LUCC, overlooking the dynamic processes during this period. Additionally, there exists a restricted research corpus concerning the influence of landscape patterns on NEP [11]. Examining how alterations in landscape patterns affect NEP facilitates the development of more efficient land management tactics, fostering favorable advancements in carbon balance. Consequently, it is vital to examine the consequences of land use alteration trends on the carbon storage capability of terrestrial ecosystems.

China strives to implement rigorous policy initiatives in the forthcoming four decades, with the target to reach a peak in CO<sub>2</sub> emissions by 2030 and achieve CO<sub>2</sub> neutrality by 2060. This is imperative for promoting sustainable ecological advancement and alleviating the repercussions of climate change [12]. However, climate change can directly impact photosynthesis and respiration within terrestrial ecosystems. Alterations in temperature, precipitation, and CO<sub>2</sub> concentrations can influence plant growth and photosynthesis rates, subsequently affecting the ecosystem's carbon absorption capacity [13]. Climate change has the potential to alter factors like soil moisture, temperature, and microbial activity. These changes can subsequently impact the rate of ecosystem respiration and organic matter decomposition, consequently influencing its capacity for carbon sequestration [14]. Examining the impacts of climate variations on NEP enables us to enhance our comprehension of how ecosystems respond to environmental fluctuations [15]. This further assists in deciphering the reaction and reciprocal mechanisms of ecosystems, directing the development of adaptation and mitigation tactics, and bears noteworthy implications for evaluating the worldwide carbon circulation and its association with climate alterations [16].

Existing research indicates that the NEP of terrestrial ecosystems has experienced significant spatiotemporal heterogeneity changes on a global scale [17]. Concurrently, while the dynamic changes of terrestrial ecosystem NEP have been monitored, most studies have utilized linear regression or the Mann–Kendall trend detection method to detect its linear trend [18], leaving its nonlinear characteristics still largely unexplored [19]. Overlooking the nonlinear features of NEP may mask the ongoing phenomena of NEP intensification and declining trend transitions [20]. Thus, understanding the nonlinear changes in NEP can help identify the key states and inflection points of ecosystems, facilitating the formulation of appropriate conservation strategies and management measures, which is crucial for guiding ecosystem management and preservation [21]. However, Empirical Mode Decomposition Ensemble (EEMD), as a nonlinear trend analysis method, possesses advantages such as adaptability, effective noise reduction, independence from prior knowledge, natural decomposition, a non-parametric nature, and multi-level decomposition integration. It can adapt to nonlinear signals with different frequencies and amplitudes, accurately extract the characteristic components of the signal (Intrinsic Mode Function (IMF)), remove noise, and

preserve the natural decomposition of the signal [22]. EEMD does not require assumptions about the signal, making it suitable for nonlinear feature extraction from various types of data without the need for predefined models or parameter settings. Through multiple decompositions and integration, EEMD provides stability and reliability [23], offering a powerful and widely applicable tool for nonlinear trend analysis.

Simultaneously, most studies analyzing the correlation of changes in terrestrial ecosystem carbon sequestration do not undergo detrending [24]. Without detrending, time series data may exhibit apparent trends, potentially leading to misleading correlation results [25]. Correlation analysis between time series without detrending can result in spurious correlations. Detrending, by eliminating trends in time series data, makes the data more stationary [26]. This makes it possible to more accurately estimate the correlation between two variables without being influenced by trends. Therefore, detrending plays a pivotal role in analyzing the connection between vegetation dynamics and climate variability [27]. While linear models are commonly used for detrending, they assume a constant trend in time series, which may yield inaccurate results in non-stationary data. As vegetation changes are inherently nonlinear, linear models may not capture their evolving trends accurately [28]. In contrast, EEMD offers an adaptive approach for analyzing non-stationary time series. EEMD's detrending method is flexible and does not rely on predetermined functional forms, making it more robust for identifying trends over time [29]. Moreover, EEMD trends are not influenced by future data, enhancing their reliability in revealing nonlinear patterns. Thus, EEMD detrending is preferable over linear methods for assessing vegetation responses to climate [30].

The Xinjiang region is a crucial hub for China's energy and economic development, yet it faces challenges in ecological and environmental conservation [31]. Exploring alterations in carbon absorption potential provides the chance to achieve an equilibrium between economic advancement and environmental conservation. Considering the fluctuations in ecosystem carbon sink capacity during the planning of development projects in energy, agriculture, industry, and transportation can aid in reducing carbon emissions, optimizing resource utilization, and promoting sustainable, green development [32]. Moreover, Xinjiang boasts extensive ecosystems, such as grasslands, forests, and wetlands, that exhibit high carbon sink capacities. Comprehending the fluctuations in ecosystem carbon sink capacity facilitates the evaluation of ecosystem health, identification of vulnerable ecosystems, and implementation of corresponding protective measures [33]. By studying the changes in carbon sink capacity, it becomes possible to evaluate the ecosystem's responsiveness to climate change, guide the formulation of adaptive measures, reduce carbon emissions, and enhance carbon absorption, ultimately mitigating the effects of climate change [34]. Focusing on the Xinjiang area in China, this investigation employs the EEMD technique to scrutinize shifts in the carbon absorption capacity of land ecosystems and the associated alterations in landscape patterns. By utilizing Pearson correlation examination, the research assesses the impact of landscape pattern modifications and temperature–precipitation data (post-EEMD detrending) on NEP fluctuations. The main objectives of this research are: (1) to scrutinize the alterations and nonlinear tendencies of NEP in Xinjiang's terrestrial ecosystems across various temporal scales; (2) to clarify the changes of land use and land cover transformations in Xinjiang; and (3) to explore the annual correlations among land use changes, meteorological alterations, and NEP through EEMD detrending analysis.

## 2. Materials and Methods

### 2.1. Study Area

The Xinjiang Uygur Autonomous Region (Figure 1), positioned in the northwest region of China, spans geographic coordinates ranging from 34°22' to 49°33' N and 73°22' to 96°21' E. Encompassing an approximate total area of  $166 \times 104 \text{ km}^2$ , it represents approximately one-sixth of China's entire land mass [35]. Situated at the core of the Eurasian continent, Xinjiang is encircled by towering mountain ranges on all sides, including the Altai Mountains, the Kunlun Mountains, and the Tianshan Mountains. Nestled within

these three mountainous regions are the extensive expanses of the Junggar and Tarim basins, which constitute Xinjiang's distinctive geographical feature, often referred to as the "three mountains surrounding two basins". Xinjiang's climate typifies the temperate continental arid climate [36]. Overall, there is a noticeable trend of decreasing temperature from the south to the north. The lower latitude areas in the south and southwest have higher temperatures, while the higher latitude regions in the north and northeast are cooler. Additionally, with increasing altitude, temperatures show a decreasing trend, resulting in colder temperatures in mountainous areas. There exists a clear disparity in the spatial distribution of annual precipitation across Xinjiang. It primarily displays a dry climate pattern in the western regions, semi-arid conditions in the east, and comparatively elevated humidity levels in the southern areas. The western regions, like the Tarim Basin and the Kurluktag Desert, receive extremely low annual precipitation, typically less than 100 mm, classifying them as hyper-arid areas. Contrastingly, the eastern regions, like the Junggar Basin and the Ili Valley, receive slightly higher annual precipitation, typically between 100 and 200 mm, placing them in the semi-arid category. Conversely, the southern regions, situated on the southern foothills of the Tianshan and Kunlun Mountains, encounter relatively higher annual precipitation, usually ranging between 200 and 400 mm, resulting in relatively moist semi-arid conditions [37].

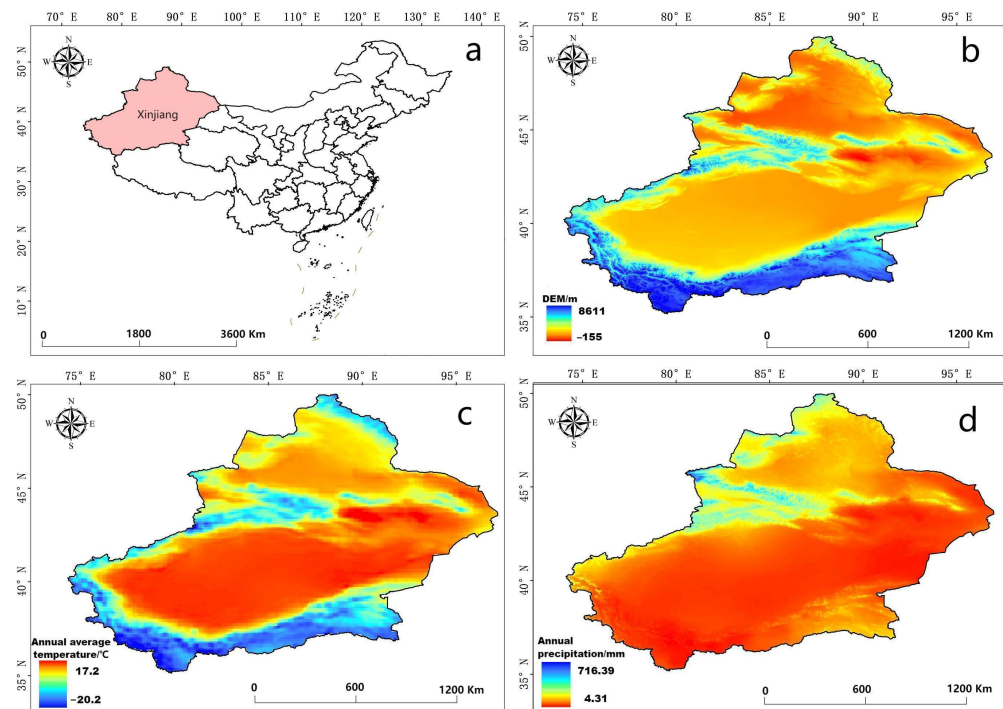


**Figure 1.** Study area overview diagram. (a): Distribution map of the study area; (b): elevation of the study area; (c): average annual air temperature in the study area; (d): average annual precipitation in the study area.

## 2.2. Data Sources

Global NEP simulations from 1981 to 2019 were collected from the National Ecological Data Center (<http://www.nesdc.org.cn>, accessed on 16 September 2023). The BEPS model was used to produce the global NEP data product for the same period using remote sensing information for vegetation parameters, atmospheric CO<sub>2</sub> concentrations, and weather data [38]. The spatial resolution of this data product is  $0.072727^\circ \times 0.072727^\circ$ .

From 1981 to 2019, the monthly average temperature grid was derived from an ERA5-Land dataset published by the European Union and European Centre for Medium-Range Weather Forecasts (<https://doi.org/10.24381/cds.68d2bb30>, accessed on 16 September 2023). It has a spatial resolution of  $0.1^\circ \times 0.1^\circ$ , representing the air temperature at 2 m

above ground [39]. For subsequent research convenience, the original data unit was converted to degrees Celsius, and its spatial extent was cropped to encompass only the Xinjiang region.

The monthly total precipitation raster data covering the period from 1981 to 2019 was obtained from a dataset shared by Peng Shouzhong on the National Tibetan Plateau Data Center platform (<https://zenodo.org/records/3114194>, accessed on 16 September 2023). With a spatial resolution of approximately 1 km, the data underwent downscaling for the Chinese region using the Delta spatial downscaling scheme. This downscaling was conducted on the basis of the CRU Global Climate Dataset of 0.5° and the World Climate High Resolution Global Climate Dataset [40]. In addition, the data were further validated with data from 496 independent weather observatories, which were considered reliable. In order to make it easier to study in the future, the original unit of the data has been transformed into mm (mm) and its spatial scope has been cut down so that it only covers the whole of Xinjiang.

Annual land use data from the Zenodo database, covering the period 1990–2019, with a spatial resolution of 30 m (<https://zenodo.org/records/4417810>, accessed on 16 September 2023) was used. The types of land use are divided into nine types: farmland, forest, shrubland, grassland, water, snow, ice, waste, water, and wetlands. The dataset was created from 335,709 Landsat images available on Google Earth Engine. All available Landsat data were used to produce various temporal indicators, which were then used in a random forest classifier to derive classification results. Through the integration of spatiotemporal filtering and logic reasoning, the spatial and temporal consistency of the proposed algorithm was improved and the overall precision of the classification reached 79.31% [41]. Considering the minimal changes in Chinese land use data before the 1990s [42], and to ensure temporal consistency between LUCC data and NEP data in the time series, 1985 LUCC data was used as a substitute for the 1981–1984 LUCC data and 1990 LUCC data was used as a substitute for the 1986–1989 LUCC data.

### 2.3. Ensemble Empirical Mode Decomposition (EEMD) Method

EEMD is a method for the decomposition of nonlinear and non-stationary signals into multiple Intrinsic Mode Functions (IMFs). It improves on the old Empirical Mode Decomposition (EMD) approach [43]. EMD is an adaptive signal decomposition technique that breaks down a signal into a sequence of Intrinsic Mode Functions (IMFs). Each IMF characterizes an inherent oscillatory mode within the signal [44]. However, EMD encounters issues of mode mixing when dealing with real signals, meaning that IMFs can interfere with each other. To address this problem, EEMD incorporates an element of randomness. It decomposes the original signal multiple times by adding various noise perturbations [45]. During each decomposition, the nature of the noise perturbation varies, resulting in slightly different IMFs for each iteration. Ultimately, the IMFs obtained from multiple decompositions are averaged, mitigating the impact of noise on the decomposition outcome [46].

The EEMD decomposition procedure is as follows:

1. Introduce a Gaussian white noise series  $w_1(t)$  into the original data  $X(t)$ . The amplitude of the Gaussian white noise series is set at 0.2 times the standard deviation of the original data [47].

$$X_1(t) = X(t) + w_1(t) \quad (1)$$

2. Connect the local maxima and minima of the time series data  $X_1(t)$  using a cubic spline to form the upper and lower envelope curves. Subtract the average  $m_1(t)$  of the upper and lower envelope curves from the time series data  $X_1(t)$ .

$$f_1(t) = X_1(t) - m_1(t) \quad (2)$$

3. Determine whether  $f_1(t)$  meets the specified condition (approaching 0 at every point). If it does, halt the sifting process. Otherwise, use  $f_1(t)$  as the new time series data and repeat step 2. This results in the first IMF:  $imf_1(t)$ .

$$\begin{aligned} f_2(t) &= f_1(t) - m_2(t) \\ imf_1(t) &= f_k(t) = f_{k-1}(t) - m_k(t) \end{aligned} \quad (3)$$

4. The residue  $R_1(t)$  is derived by subtracting  $imf_1(t)$  from  $X_1(t)$ . If  $R_1(t)$  continues to possess oscillatory components, it is then used as the new time series data and steps two and three are reiterated.

$$\begin{aligned} R_1(t) &= X_1(t) - imf_1(t) \\ R_n(t) &= R_{n-1}(t) - imf_n(t) \end{aligned} \quad (4)$$

5. Consequently,  $X_1(t)$  is decomposed into a series of Imfs with decreasing frequency and a monotonic trend with at most one extreme point.

$$X_1(t) = \sum_{i=1}^n imf_i(t) + R_n(t) \quad (5)$$

6. Step five: Repeat steps one to four 1000 times, introducing different Gaussian white noise in each iteration. The ensemble mean of all the decomposed intrinsic mode functions and long-term trends is taken as the final decomposition result [48].

In this study, we assess the statistical significance of the nonlinear trends delineated by EEMD [49]. The detailed methodology is presented as follows:

1. Generate 5000 white noise sequences of equal length to the original sequence.
2. The EEMD is used to decompose each generated white noise series to extract their long-term trends (IMF).
3. Each extracted long-term trend is divided by the original data standard deviation and the normalized trend is obtained.
4. For each normalized trend, determine the number of extrema. If the count of the extrema is zero, proceed to step 5; if there is one extremum, proceed to step 6.
5. Determine if trend values exceed the confidence interval:
  - a. Identify the corresponding range for the trend of the added white noise sequences at a 95% confidence level, which is 1.96 times the standard deviation.
  - b. For the normalized trend, evaluate whether it falls outside the confidence interval. If it does, the trend is considered significant; otherwise, it is deemed not significant.
6. Identify inflection points:
  - a. Locate the inflection points within the normalized trend, which are the extrema.
  - b. Before the inflection point, execute step 5.
  - c. After the inflection point, compute the difference in trends divided by the standard deviation and then proceed to step 5.

On the basis of the significance of EEMD trends, the nonlinear trends of EEMD fall into five categories (Table 1).

**Table 1.** The nonlinear trend of the EEMD.

Type	Description
No significant change	the trend is not significant in any year
Monotonic increase/decrease	the trend exhibits a monotonic increase/decrease with statistical significance in at least one year
Initial increase then decrease/initial decrease then increase	the trend initially increases and then decreases/decreases and then increases, including a local maximum/minimum, with statistical significance in at least one year

#### 2.4. Pearson Correlation Analysis

Pearson correlation examination is a statistical method utilized to measure the linear connection between two factors [50]. This association is measured utilizing the correlation coefficient, marked as “ $r$ ”, which spans from  $-1$  to  $1$ . A value of “ $r$ ” nearer to  $1$  or  $-1$  shows a more robust correlation, whereas an “ $r$ ” close to  $0$  proposes minimal to zero linear connection between the factors. The symbol of “ $r$ ” signifies the direction of the correlation: a positive value indicates a favorable correlation, whereas a negative value indicates an adverse correlation. The equation to compute the correlation coefficient  $r$  is:

$$r = \frac{\sum (X - \bar{X})(Y - \bar{Y})}{nS_X S_Y} \quad (6)$$

$$S_X = \sqrt{\frac{\sum (X - \bar{X})^2}{n - 1}} \quad (7)$$

$$S_Y = \sqrt{\frac{\sum (Y - \bar{Y})^2}{n - 1}} \quad (8)$$

In the formula,  $S_X$  and  $S_Y$  represent the standard deviations of variables  $X$  and  $Y$ , respectively, and  $n$  signifies the sample size.

Moreover, the  $p$ -value is frequently utilized to assess the significance of the correlation coefficient, determining whether the correlation genuinely exists or may be attributable to random factors. Typically, if the  $p$ -value is less than a predefined significance level, the correlation coefficient is deemed statistically significant [51].

In this investigation, we first utilized the EEMD approach to remove trends from both the NEP and meteorological information. Subsequently, we utilized Pearson correlation examination to explore the relationships among various meteorological variables and NEP. To quantitatively assess the impact of diverse meteorological variables on NEP, we chose the meteorological variable with the greatest squared correlation coefficient (the determination coefficient,  $r^2$ ) for each pixel, recognizing it as the principal climatic factor influencing vegetation in that pixel [52].

#### 2.5. Land Use Patterns Analysis

Landscape metrics are utilized as tools to evaluate and dissect land use configurations, providing insights into the spatial dispersion and organizational characteristics of various land use categories [53]. They offer quantitative representations of compositional attributes, spatial allocation, and the dynamic transformations occurring within land use patterns. In this study, the Fragstats 4.2.1 software’s mobile window method was employed to calculate landscape indices using time series land use data for Xinjiang spanning from 1981 to 2019. When determining landscape configuration indices, it is crucial to consider three key factors: the features of the landscape elements, the spatial layout of the landscape components, and the overall diversity of the landscape [54]. With a focus on quantifying landscape metrics to capture shifts in landscape configurations and evaluating their correlation with NEP, six representative indices were carefully selected, taking into account the specific circumstances of this investigation.

1. Patch Density (PD): PD quantifies both the quantity and distribution density of patches for a specific land use type. A higher patch density indicates a greater number of dense patches, whereas a lower patch density implies fewer and more scattered patches;
2. Largest Patch Index (LPI): LPI assesses the size of the largest contiguous patch within a land use type. Higher LPI values indicate larger contiguous patches, while lower values suggest smaller ones;
3. Area Weighted Mean Patch Fractal Dimension (AWMPFD): AWMPFD evaluates the complexity of patches within a land use type. Higher AWMPFD values indicate more complex patch shapes, while lower values suggest simpler ones;

4. Contagion (CONTAG): Contagion reflects the degree of spatial separation between different land use types. A higher index indicates relative separation, while a lower index suggests a more mixed distribution;
5. Shannon's Diversity Index (SHDI): SHDI measures the diversity and evenness of land use types. Higher SHDI values indicate greater diversity, while lower values suggest less diversity;
6. Modified Simpson's Evenness Index (MSIEI): MSIEI measures the evenness of distribution between different land use types. Higher MSIEI values indicate a more even distribution, while lower values suggest uneven distribution.

These indices can be utilized to assess various aspects of land use patterns, including patch quantity, size, shape complexity, spatial separation, diversity, and evenness [55]. Through the calculation and comparison of these indices, quantitative insights into land use patterns can be derived. This process facilitates the exploration of relationships between different land use types, spatial distribution characteristics, and their ecological implications (Figure 2).

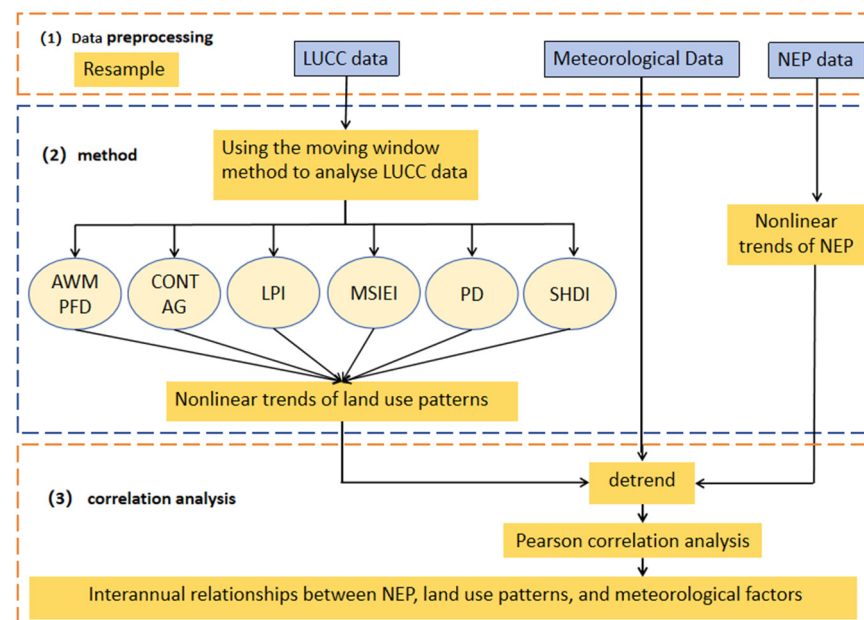


**Figure 2.** Technical lines of research.

### 3. Results

#### 3.1. Multi-Time Scale Variations of the NEP in the Terrestrial Ecosystems of Xinjiang

At the regional scale, the Net Ecosystem Productivity (NEP) was decomposed into five Intrinsic Mode Function (IMF) components and one upward trend, as illustrated in Figure 3. The average periods for these five IMF components are 3, 5, 7, 16, and 34 years, as shown in Table 2. Among them, IMF1 has the largest average variance contribution, accounting for 42.8%, followed by IMF2. Thus, NEP is more susceptible to external disturbances on shorter time scales. Concurrently, with a variance contribution rate exceeding 10% on a 7-year time scale, the interannual variability is also noteworthy and should not be ignored.

On the 3-year time scale, areas along the northern foot of the Tianshan Mountains, especially regions like Tacheng, Changji, and Bozhou, which are primarily characterized by alpine meadows and grasslands, as well as regions like Yili, Altay, and Urumqi, where grasslands, alpine meadows, wetland vegetation, and coniferous forests dominate, exhibit variance contribution rates exceeding 37% (Figure 4a).



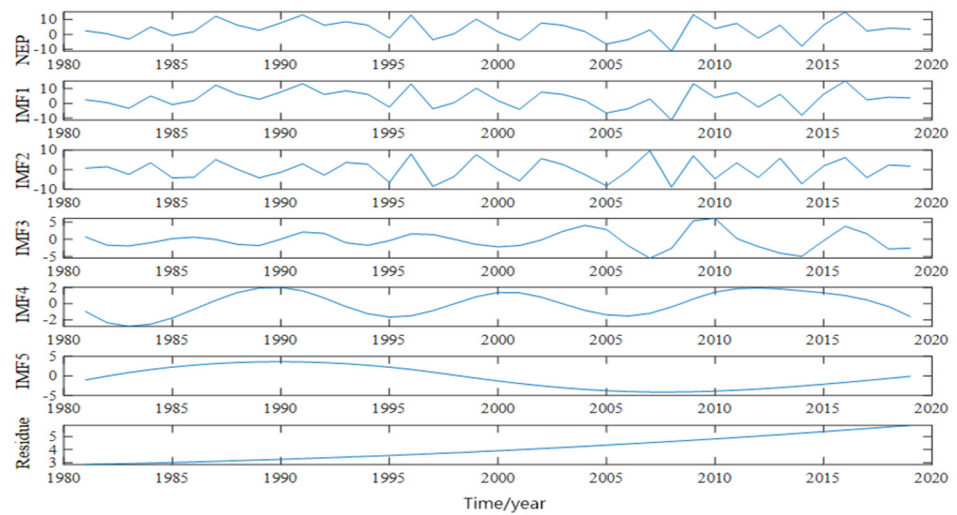


**Figure 3.** EEMD analysis of the average NEP changes during 1981–2019. IMF1–IMF5 and residue representing variations on different time scales and long-term trend, respectively.

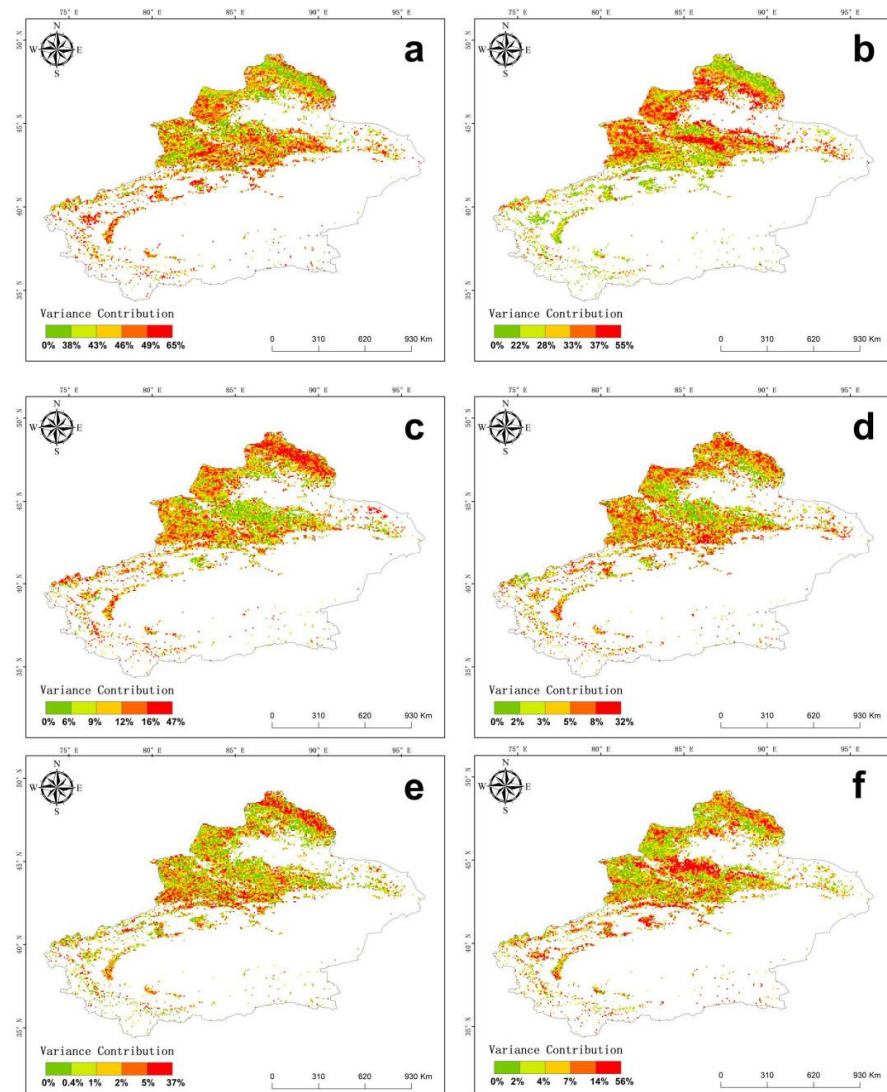


**Figure 4.** Spatial distribution of the variance contribution rates of different time scales to NEP changes, classified using 20% quantiles: (a) 3-year time scale, (b) 5-year time scale, (c) 7-year time scale, (d) 16-year time scale, (e) 34-year time scale, and (f) long-term trend.

**Table 2.** Variance contribution rate (VC, %) and average period (year) of the average NEP change of all pixels on different time scales.

Variable Types	Statistical Indicators	IMF1	IMF2	IMF3	IMF4	IMF5	Residue
Period	Mean	3	5	7	16	34	-
	Std	0.3	0.6	1.3	6.3	8.1	-
Variance Contribution	Mean	42.8	29.7	11.2	5.5	2.7	8.1
	Std	8.2	6.7	6.2	4.3	4.0	8.6

On the 5-year time scale, areas with variance contribution rates surpassing 49% are mainly concentrated around the northern slope urban clusters of the Tianshan Mountains, characterized by coniferous forest belts, meadow grasslands, mountain shrubs, and valley wetlands (Figure 4b).

On the 7-year, 16-year, and 34-year time scales, the spatial distribution of variance contribution rates is largely consistent (Figure 4c–e). The primary areas with higher variance contribution rates are in the northern regions of Altay and Tacheng, as well as in areas like Yili, Bozhou, and the Hejing County of Bazhou.

For the long-term trend, regions like Changji, Urumqi, the southern part of Tacheng, and the northern part of Altay exhibit change contribution rates exceeding 14%. This suggests that the long-term trend also has a notable impact on the variations in NEP in certain areas of Xinjiang (Figure 4f).

In summary, the Net Ecosystem Productivity (NEP) in the northern foothills of the Tianshan Mountains in Xinjiang exhibits susceptibility to interannual variations. Across the entire study region, fluctuations on the 3-year and 5-year time scales play a predominant role in driving variations in NEP.

### 3.2. Spatial Distribution of the Nonlinear Trend in NEP for the Terrestrial Ecosystems of Xinjiang

The majority (53.32%) of the NEP trends exhibit no significant variations and are predominantly located in the northern sector of the study area (Figure 5), characterized primarily by grassland vegetation. Given the climatic and geographical conditions of this region, grasslands emerge as one of the most favorable vegetation types. These grasslands span vast expanses, encompassing extensive areas of alpine meadows and temperate grasslands. Additionally, in regions experiencing notable changes in NEP, the dominant vegetation types comprise coniferous forests, meadows, mountain shrubs, and riparian wetlands, which are predominantly clustered around the northern slopes of the Tianshan Mountains urban cluster. The observed trend often manifests as an initial decrease followed by a subsequent rise, constituting roughly 35% of the total observed changes. This indicates significant potential for ecological restoration in the area, hinting at a possible deceleration in the declining NEP trend and even a potential shift towards an increasing trend. Furthermore, although the proportion of areas exhibiting a consistent decline in NEP is relatively minimal (1.59%), those showing an initial increase followed by a subsequent decline reach 4.49%. This underscores the vulnerability of the ecosystems in these regions to degradation following initial recovery efforts.

### 3.3. Nonlinear Trends of the Changes in Land Use Pattern in Xinjiang over the Last 40 Years

The Ensemble Empirical Mode Decomposition (EEMD) technique was utilized to conduct trend analysis on six key indices of land use patterns, revealing nonlinear trends within Xinjiang over the past four decades. Examination of each landscape index indicated that only a small portion of the region had insignificant land use changes, suggesting substantial overall alterations in land use patterns across most areas of the region. Specifically, PD exhibits a consistent increase with fluctuations (Figure 6d), implying a growing trend of patch density and fragmentation. Conversely, the LPI generally displays a pattern of increase followed by decrease, accompanied by a steady decline (Figure 6b), indicating a reduction in the maximum patch area. The AWMPFD demonstrates a trend of decrease,

followed by increase and a steady rise (Figure 6a), implying an increase in patch shape complexity. However, the contagion index predominantly shows an initial increase, followed by a decrease and a steady decline (Figure 6f), suggesting reduced patch aggregation and connectivity. The SHDI results show the highest proportion of areas experiencing an increase to decrease or showing a steady rise (Figure 6e), reflecting a significant rise in land use diversity and complexity. MSIEI indicates a prevailing trend of an initial decrease followed by an increase, with a steady decline (Figure 6c), suggesting a general increase in land use type evenness, albeit with regional variations.

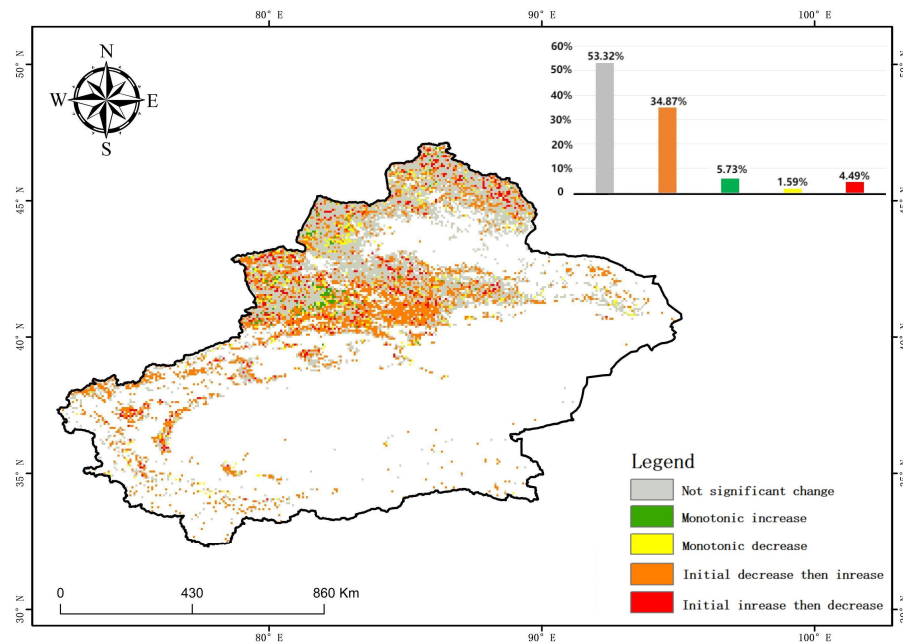


**Figure 5.** Nonlinear trends of NEP changes in Xinjiang from 1981 to 2019.

In general, the fragmentation and shape complexity of the patch generally increased, with a reduction in patch connectivity and the size of the largest dominant patch. Additionally, there is an increase in the diversity and evenness of land use types. However, the changes mostly involve non-monotonic trends with transitions.

### 3.4. The Correlation between NEP and Land Use Patterns

In order to study the annual relationship between land-use patterns and NEP in space, we used nonlinear detrending techniques to remove trends and extract annual variations in NEP and land use patterns. Then, a Pearson correlation analysis was performed to reveal the potential relationship between the NEP and land use patterns. Our research indicates that, except for MSIEI, which primarily exhibits a positive correlation with NEP, the proportions of areas demonstrating positive and negative correlations between other pattern indices and NEP are comparable (Table 3).

**Table 3.** Area percentages of Correlation between pattern of land use and NEP (%).

	AWMPFD	LPI	MSIEI	PD	SHDI	CONTAG
$r > 0, p > 0.05$	39.4	59.9	46.9	38.7	41.1	36.5
$r > 0, p < 0.05$	5.1	20.7	10.1	5.8	5.3	4.5
$r < 0, p > 0.05$	46.6	18.3	37.4	45.9	45.9	47.4
$r < 0, p < 0.05$	8.9	1.1	5.5	9.6	7.7	11.6

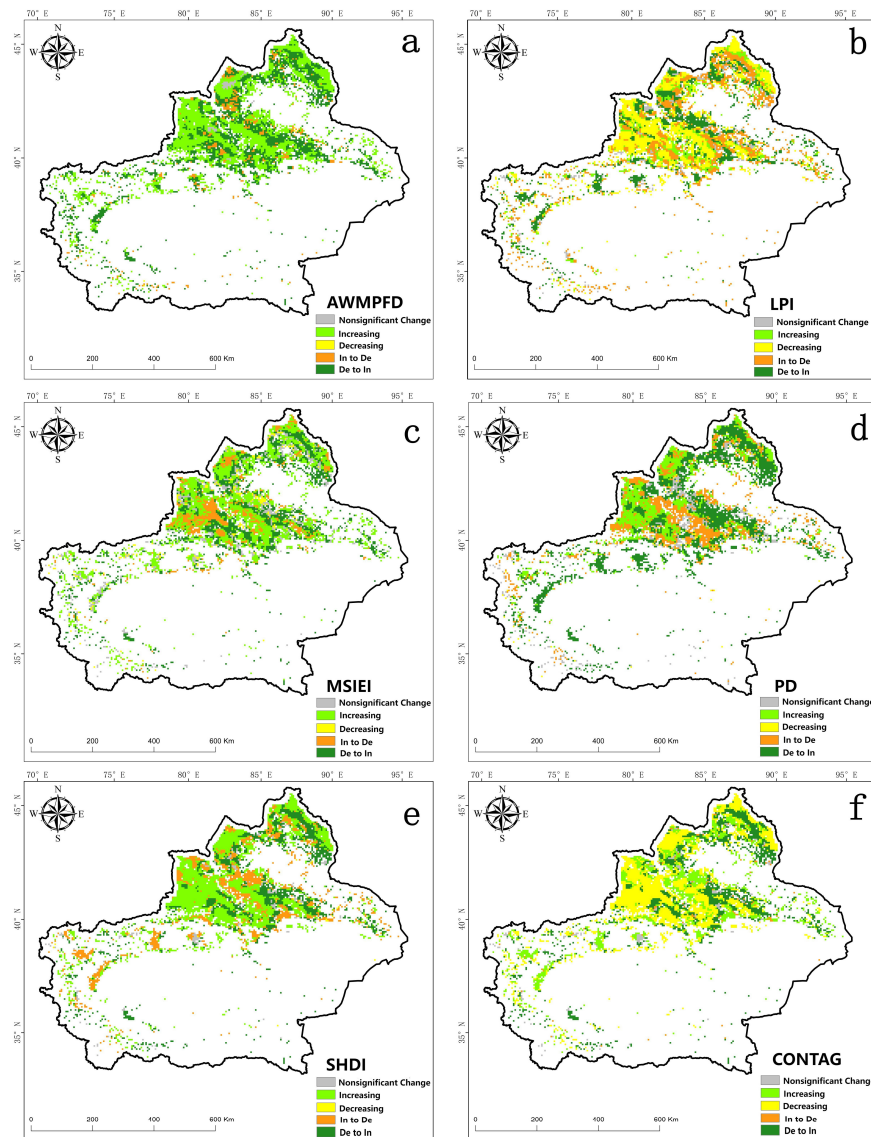


**Figure 6.** Spatial distribution of land use pattern changes in Xinjiang from 1981 to 2019: (a) AWMPFD, (b) LPI, (c) MSIEI, (d) PD, (e) SHDI, and (f) CONTAG.

In regions exhibiting notable correlations, AWMPFD, PD, SHDI, and CONTAG demonstrate significant negative correlations with NEP (see Figure 7a,d,e,f), whereas MSIEI and LPI show significant positive correlations with NEP (Figure 7b,c). This indicates that the complexity of the patches, fragmentation, the variety of land use types, and the clustering of patches hinder the growth of the NEP, whereas the greater the uniformity of the patch and the dominant patch area, the greater the NEP.

### 3.5. The Correlation between NEP and Meteorological Changes

Utilizing detrended NEP data and meteorological information processed with EEMD, we conducted a comprehensive analysis using Pearson's method on a pixel-by-pixel basis to unveil the inter-annual relationship between climate change and NEP, particularly concerning spatial patterns. Table 4 presents the analysis results regarding the spatial distribution correlation between NEP in Xinjiang over the past 40 years and temperature and precipitation. It is evident that the spatial correlation of NEP with temperature varies across different regions (Figure 8a). Positive correlation is observed in 62% of areas, with 33% exhibiting significant positive correlations, mainly concentrated in the Tianshan mountains and the Kunlun mountain range. Conversely, negative correlation is noted

in 38% of regions, with significant negative correlation covering 22% of the total area, primarily in vast plains and desert regions. Regarding the spatial correlation of NEP with precipitation, it is predominantly positive in 95% of areas (Figure 8b), with 83% showing significant positive correlation, while only 5% exhibit negative correlation.

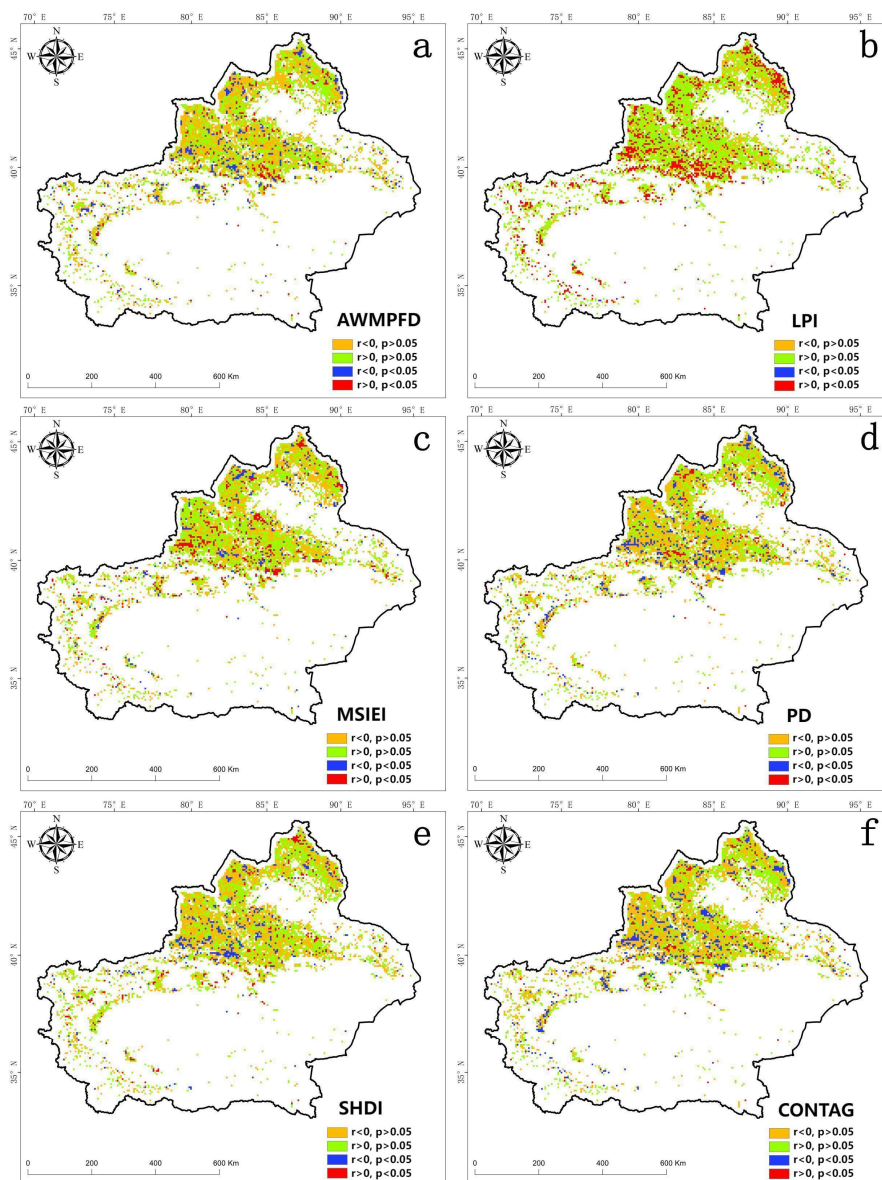


**Figure 7.** Interannual relationship between NEP and land use patterns: (a) AWMPFD, (b) LPI, (c) MSIEI, (d) PD, (e) SHDI, and (f) CONTAG ( $r$ : correlation coefficient;  $p$ : significance level).

**Table 4.** Area percentage of the correlation between air temperature or precipitation and NEP (%).

	Temperature	Precipitation
$r < 0, p > 0.05$	16.08	4.01
$r > 0, p > 0.05$	28.99	12.17
$r < 0, p < 0.05$	21.85	1.15
$r > 0, p < 0.05$	33.08	82.69

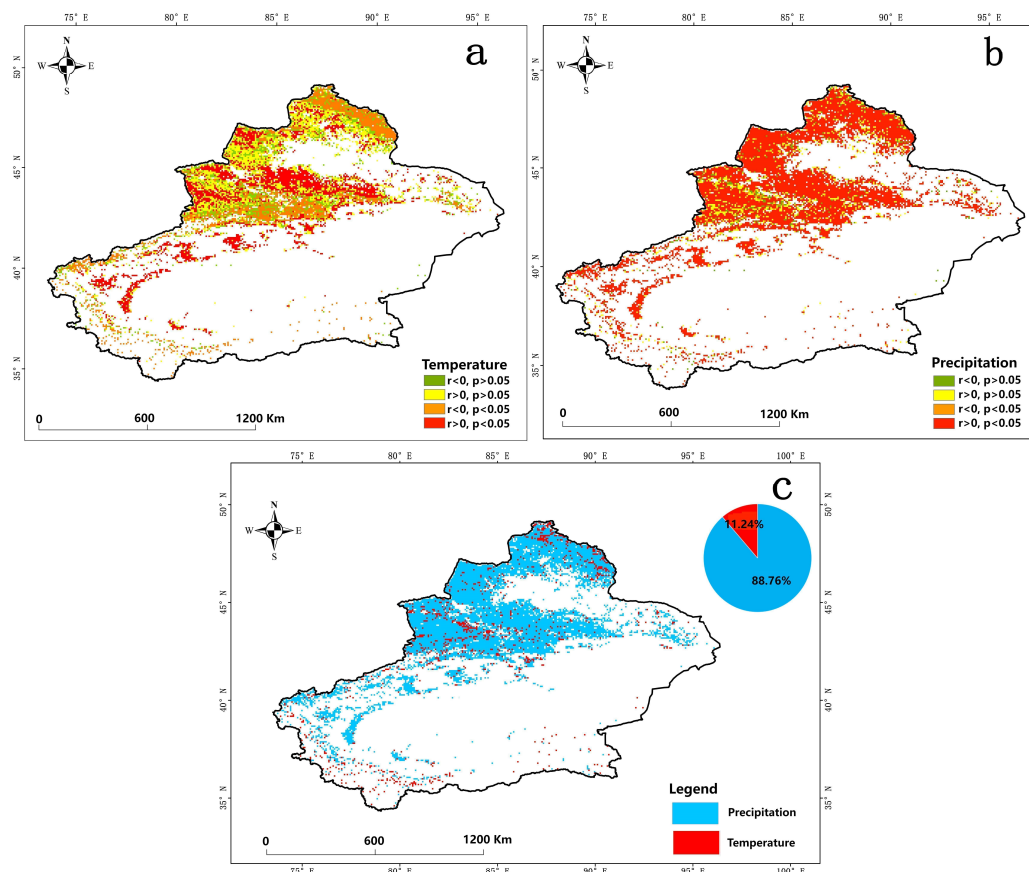


**Figure 8.** Interannual relationship between NEP and temperature (a) or precipitation (b) ( $r$ : correlation coefficient;  $p$ : significance level) and spatial distribution of key climatic factors affecting NEP in the Xinjiang (c).

Analyzing the distribution area of key climate factors (Figure 8c), it is evident that the regional NEP is primarily positively correlated with precipitation, whereas its correlation with temperature is comparatively weaker. Precipitation impacts the largest area (88%), while the influence of temperature covers only 12% of the region. This suggests that changes in Xinjiang's NEP are more responsive to precipitation variations. A rising trend in precipitation positively contributes to the local NEP.

#### 4. Discussion

##### 4.1. Variations in the NEP on Multiple Time Scales

At the regional scale in Xinjiang, variations in NEP primarily follow a 3-year cycle, with a variance contribution rate of 42.8%. The annual NEP demonstrates a trend of short-term fluctuating growth. Simultaneously, cyclical changes on a 5-year scale have a significant contribution to NEP, accounting for 29.7% of the total. Areas affected by these short-term scale fluctuations are mainly located in the northern foothills of the Tianshan mountains, with vegetation predominantly consisting of alpine meadows and grasslands [56]. The carbon flux and its components in the alpine meadow ecosystems are highly sensitive to grassland degradation [57]. Due to their high-altitude locations, they possess a shorter growing season [58]. This suggests that short-term adverse climatic events, such as persistent low temperatures or snowfall, could have detrimental effects on the entire growing season of the vegetation [59]. Furthermore, the root structures of vegetation in alpine meadows and grasslands are typically fragile. Plants in these ecosystems often have shallow and underdeveloped root networks unable to efficiently shield the soil and vegetation from disturbances [60]. Consequently, these systems, when subjected to short-term disruptions, may experience alterations in soil texture and moisture distribution,

subsequently affecting the growth and survival conditions of plants [61,62]. However, these ecosystems can also be impacted by human activities such as grazing, agriculture, and wastewater discharge. These short-term human-induced interferences can rapidly alter the vegetation structure and ecological functions of the region [63].

In summary, alpine meadows and grasslands are especially susceptible to environmental fluctuations over short time frames due to their heightened sensitivity to such changes, coupled with the fragility of their vegetation's root structures, alterations in soil texture and moisture, and human interventions. These factors make these ecosystems particularly vulnerable to disturbances over a 3–5-year short-term span. As such, the protection and management of these ecosystems should take these factors into account, implementing appropriate measures to reduce the negative impacts of short-term disturbances on vegetation and thereby promoting their recovery and sustainable progression.

In addition, the distributions of the long-term variations on the 7-year, 16-year, and 34-year time scales and the long-term trend are similar. They are primarily concentrated in the northern regions of Altay and Tacheng, as well as in areas such as Ili, Bortala, and the Hejing county of Bayingol. These regions predominantly feature coniferous forests, desert vegetation, and cultivated lands [64]. Due to their characteristics, they are more susceptible to long-term inter-annual changes rather than short-term disturbances. Coniferous forests, for instance, typically possess longer lifecycles and slower growth rates, enabling them to better adapt to sustained environmental shifts. Short-term environmental changes, such as mild droughts or brief temperature fluctuations, may not immediately inflict significant harm upon them [65]. On the other hand, desert vegetation has evolved to withstand the pressures of extreme conditions, including high temperatures, droughts, and intense sunlight. This adaptive capacity enables them to resist short-term environmental oscillations. As a result, these types of vegetation tend to have a higher resilience to short-term environmental fluctuations [66]. Whereas certain brief disturbances might harm these ecosystems, they exhibit a relatively strong ecological recovery capability and the adaptability to withstand a degree of natural change and environmental stress. Moreover, under human management, farmlands are less susceptible to short-term disturbances, ensuring a relatively stable ecosystem [67].

Nevertheless, it is crucial to recognize that even relatively stable vegetation and agricultural lands can be influenced by natural elements and human activities. Prolonged or accumulated short-term disturbances might gradually exert their effects on them [68]. Hence, the protection and management of these ecosystems remain of the utmost importance.

#### *4.2. Spatial Distribution of the Nonlinear Trend of the NEP*

Since the 1980s, particularly after the year 2000, the vegetation coverage in most parts of Xinjiang has seen a notable improvement [69]. However, the study indicates that in 53.32% of regions, the alteration in NEP is insignificant; these regions are predominantly located in the northern section of the study area. This indicates that an increase in vegetation greening does not necessarily lead to an increase in carbon sequestration. One potential reason could be the overall arid nature of Xinjiang, especially in its northern regions. Even if vegetation cover expands, an absence of a corresponding increase in water resources might hinder the growth in ecosystem productivity [70]. The greening of the vegetation might be a result of policies like converting cultivated land back to forests and ceasing grazing to restore grasslands. However, the productivity of newly afforested areas might not surpass that of agricultural lands.

Meanwhile, the study found that 46.68% of the regions in Xinjiang exhibited significant changes in NEP. The areas with significant changes are mainly distributed in the northern part of Xinjiang, especially in the urban clusters on the northern slope of the Tianshan Mountains. However, within these areas with significant changes, the NEP exhibited different trends, including monotonic increases, initial decreases followed by increases, and sustained decreases. Although the ecological environment in Xinjiang is generally on a favorable developmental trajectory, there are evident phased fluctuations. Thus, a mere

linear trend cannot adequately capture the nonlinear characteristics inherent to the shifts in NEP's trends [71].

The EEMD method employed in this study further exposes the trend shifts in NEP changes over the past 40 years in China's terrestrial ecosystems. Upon EEMD analysis, it was discovered that only 5.73% of the regions exhibit a monotonically increasing trend, while 34.87% demonstrate an apparent trend of decreasing first and then increasing; these are primarily located in the urban clusters on the northern slope of the Tianshan mountains. This is attributed to the relatively favorable geographical conditions of the Tianshan northern slope, which is characterized by a more humid climate and superior soil quality that is conducive to the healthy development of ecosystems [72]. Compared to other regions of Xinjiang, the water resource management of the Tianshan northern slope urban clusters might have benefited from more optimized strategies and technologies, thereby maintaining ecological equilibrium more effectively [73]. The multitude of ecological restoration and afforestation projects implemented in the northwest region aim to rejuvenate degraded lands and increase vegetation cover, leading to a consistently rising trend in the ecosystem's NEP. However, with urbanization and agricultural progression, most regions might have undergone land use changes, like transitioning from natural vegetation to agricultural or construction lands [74]. This might result in a short-term decline in NEP. Subsequently, with the enforcement of ecological restoration and management measures, NEP again exhibits a rising trend.

In terms of influencing factors, the Xinjiang region has witnessed considerable land use transformations, such as urbanization, industrialization, and agricultural expansion [75]. Initially, these developments might have positively impacted the ecosystem, for instance, by enhancing agricultural productivity through irrigation. However, these advancements subsequently resulted in issues like land degradation, water scarcity, and ecological degradation [76], inducing a prominent "rise-then-fall" trend in 4.49% of the areas. Additionally, Xinjiang, characterized by its arid nature, has seen a spike in water demand due to the expansion of agriculture and industry, potentially leading to moisture deficits in specific ecosystems. Factors like excessive grazing and ill-advised agricultural practices further exacerbate land degradation [77], resulting in a consistently decreasing trend in NEP across 1.59% of the regions.

However, these trend shifts highlight the complexity and dynamism of ecosystem evolution, which does not always follow a straightforward linear model. Both restoration and degradation can coexist. Therefore, unlike the linear trend analysis of NEP, nonlinear trend analysis enables the exploration of hidden restorative potential and the potential risks of degradation. It reveals the true trajectory of NEP changes, aiding in a more thorough assessment of Xinjiang's terrestrial ecosystems' carbon sink capacity and evolving patterns.

#### *4.3. Nonlinear Trends of the Changes in Land Use Pattern*

Since the late 1980s, China's land use change has exhibited significant spatiotemporal heterogeneity [78]. This study reveals significant changes in the landscape pattern of Xinjiang, China, which is characterized by increased dispersion, complexity, diversity, and uniformity. Previous research has noted changes in land use patterns, highlighting a growing level of both fragmentation and aggregation. However, these studies often concentrate on specific or short-term changes in land use patterns, overlooking long-term trends in landscape patterns [69].

This study shows that PD, AWMPFD, SHDI, and MSIEI trends are predominantly rising, whereas LPI and CONTAG display mainly declining trends. This indicates an overall rise in patch fragmentation and shape complexity, alongside an increase in the diversity and uniformity of land use types. Examining the developments in Xinjiang over the past four decades, the shifting trends in landscape indices offer vital insights into the evolution of land use patterns.

The rise in PD suggests increased complexity in land use across Xinjiang, with patches becoming more densely distributed spatially. This could stem from human activities



like urbanization and agricultural expansion, causing greater fragmentation of land use types. AWMPFD's increase may indicate a reduction in the average size of land use patches, possibly due to urban expansion and farmland fragmentation creating more transitional areas between land use types. The uptick in SHDI implies growing diversity in Xinjiang's land use pattern over time, likely influenced by shifts between different land use types. MSIEI's rise suggests increased complexity in land use patch shapes, possibly influenced by human activities making land use type boundaries more intricate. Conversely, LPI's decline signifies heightened overall patch fragmentation, while CONTAG's decrease reflects diminished contrast between land use patches. Both declines imply increased patch fragmentation, indicating reduced clustering of land use patches and less distinct boundaries. In summary, these trends likely result from various factors such as urban expansion, agricultural activities, and land use policies shaping Xinjiang's landscape over the past four decades.

In recent years, the accelerated urbanization in the northern foothills of the Tianshan Mountains may have led to changes in land use structure [32]. Urban expansion and construction may result in the destruction and fragmentation of the original ecological landscape, leading to an increasing trend in landscape indices such as PD, AWMPFD, SHDI, and MSIEI. Meanwhile, agriculture is one of the main economic activities in Xinjiang [79], and frequent agricultural activities may lead to changes in land use types, such as the expansion of cultivated land and adjustments to farmland structures, affecting landscape patterns. These changes may manifest as an increasing trend in landscape indices. Adjustments to land use policies by the government may affect the development direction of agriculture and urbanization. Changes in policies may lead to the adjustment of land use structures, subsequently affecting landscape patterns. However, the above changes may have profound impacts on the structure and function of ecosystems [80]. Increased urbanization and agricultural activities may disrupt the original ecological balance, leading to an increase in the complexity of the ecosystem that is reflected in the increase in the four landscape indices. Conversely, the decrease in LPI and CONTAG indicates a weakening of the original ecological connectivity and uniformity, possibly due to changes in land use type and human disturbance.

#### *4.4. Interannual Relationship between Land Use Patterns and NEP*

Previously conducted research has indicated that land use patterns also influence the variation of Net Ecosystem Production (NEP). Urbanization, for instance, has led to a carbon source shift in certain regions, whereas afforestation and reforestation contribute to increased carbon sinks [81]. In the current study, it was noted that the LPI and the MSIEI show primarily positive correlations with NEP, implying that an expansion in the area of dominant patches and a uniform distribution of patches aid in augmenting NEP. Conversely, the CONTAG, along with the AWMPFD, SHDI, and PD, demonstrate significant negative correlations with NEP. This suggests that high land use type aggregation, fragmentation, diversity, and shape complexity impede the increase in NEP.

The Xinjiang region has relatively low forest coverage, with forest patches typically being small and dispersed [82]. However, forests generally possess high carbon sequestration capabilities and the forests in the natural vegetation of Xinjiang are crucial carbon reservoirs, with an annual carbon storage of 176.02 million tons [83]. During the preceding four decades, initiatives aimed at ecological safeguarding and rehabilitation, encompassing the sustained execution of natural forest preservation and afforestation endeavors, have elevated the forested expanse to 120 million hectares, attaining a forest coverage proportion of 5.02% in Xinjiang [84]. This has led to an improvement in both LPI and MSIEI by increasing the forested area and improving forest structure. Simultaneously, the fragmented boundaries of forest patches have become more complex, resulting in higher MSIEI values. This improvement likely includes adjustments to the size and distribution patterns of forest patches to promote biodiversity, species migration, and ecosystem stability. The positive

correlation indicates that positive outcomes have been achieved in terms of ecological conservation and restoration.

On the other hand, regarding the CONTAG index, which measures the degree of mixture between different land types, non-forest land types tend to have higher degrees of mixture, resulting in lower CONTAG values. The AWMPFD index, which assesses the self-similarity and fractal characteristics of patches, is generally higher for non-forest land types due to their varied forms and structures. The SHDI index, used to measure landscape diversity, is typically higher for non-forest land types. The PD index, representing the number of patches per unit area, is generally higher for non-forest land types with higher patch densities [85]. Landscape indices such as CONTAG, AWMPFD, SHDI, and PD may be closely associated with non-forest land types (such as grasslands, deserts, or farmland) and regions with lower carbon sequestration capabilities, resulting in a negative correlation with terrestrial carbon sinks.

Human activities and land use practices in Xinjiang can have a significant impact on landscape configurations and carbon sequestration. For example, large-scale farming, urban sprawl, and land fragmentation can result in the fragmentation of the landscape, which may have a negative impact on the connectivity of habitats and vegetation and eventually lead to a reduction in carbon sequestration [86]. Indicators such as the MSIEI and LPI reflect habitat connectivity and integrity. Higher LPI and MSIEI values indicate that larger and more interconnected habitat patches are present, facilitating species migration and gene flow. This improved connectivity is critical in maintaining the integrity and functionality of the ecosystem, thereby enhancing carbon sequestration.

#### 4.5. Interannual Relationship between NEP and Meteorological Changes

Climate change is a primary factor causing spatial-temporal disparities in NEP, especially in a country like China, which encompasses diverse geographic environments and spans multiple climatic zones [87]. Due to geographical, climatic, and ecological differences between northern and southern China, there are significant disparities in ecosystems' responses to climatic factors [88,89]. In the humid regions south of the Yangtze River, ample annual rainfall reduces moisture constraints and temperature variations (especially during the growing season) largely determine plant growth periods and productivity [90]. Conversely, in the arid and semi-arid regions of the northeast and northwest, limited precipitation makes moisture the predominant factor constraining plant growth and ecosystem productivity [91].

Over the past century, both temperature and precipitation in China have been on an upward trajectory, especially in the northwest, where the rise in precipitation over recent decades has been notably pronounced, steering the region towards a warmer and wetter climate trend [92]. Vegetative growth is intrinsically tied to climatic factors [93,94]. The vegetation in most parts of Northwestern China is better adapted to the local trend of increasing warmth and humidity, which is conducive to plant growth [95].

Numerous studies currently indicate that Xinjiang's climate is transitioning from warm-dry to warm-wet and, with grasslands as the predominant vegetation type in Xinjiang, the increase in precipitation could potentially stimulate grassland growth [96]. The study findings reveal that approximately 62% of regions in Xinjiang exhibit a positive correlation between NEP and temperature, with 33% demonstrating a significant positive correlation. Nearly 95% of areas show a positive correlation between NEP and precipitation, with 83% displaying a significant correlation. The spatial distribution variations in Xinjiang are primarily attributed to the sensitivity of vegetation to changes in precipitation. This is attributed to Xinjiang's location in the northwest of China, which is characterized by arid to semi-arid climatic conditions, with higher average temperatures and limited rainfall. Given that moisture is the pivotal factor restricting grassland growth, increased precipitation can bolster soil moisture supply for vegetation, enhance photosynthetic rates, and subsequently bolster the carbon sequestration capabilities of vegetation. Compared to this, the impact

of temperature changes on the NEP is relatively minor, possibly because the vegetation in Xinjiang is better adapted to the gradually warming and humidifying local climate trend.

The future adaptation of NEP in the Xinjiang region to changes in precipitation is a complex and critical issue for ecosystems. The impact of precipitation changes on NEP primarily occurs through influences on plant growth, soil moisture, and the carbon cycle within ecosystems [97]. Effective soil moisture management is crucial for maintaining the water supply to vegetation ecosystems. This may involve implementing measures to reduce soil evaporation, enhance soil water retention, and improve water use efficiency. Simultaneously, the implementation of scientific ecosystem management measures, such as vegetation restoration, soil and water conservation, and rational land use planning, can assist in enhancing the stability of ecosystems, enabling better adaptation to changes in precipitation levels [98]. The establishment of a comprehensive monitoring system that provides real-time data on precipitation, vegetation growth, and other factors is essential for an early warning of future changes, facilitating timely adjustment measures. Public engagement and community collaboration are also pivotal strategies for addressing precipitation changes. Through education and cooperative efforts, awareness of environmental changes can be heightened, fostering the implementation of sustainable development practices. It is important to note that a comprehensive understanding of future precipitation changes requires the consideration of climate model predictions, region-specific ecosystem characteristics, and human activities. Therefore, interdisciplinary research and cross-sector collaboration are key to formulating effective adaptation strategies.

In summary, our research highlights the impact of climate change on NEP, with a particular emphasis on the significant influence of precipitation fluctuations. This finding holds important practical implications for understanding ecosystem responses to climate change and offers valuable insights for future predictions and adaptations in the face of changing climate conditions. Through an exploration of the ecological mechanisms underlying the NEP, our study contributes to a more profound understanding and provides guidance for future ecosystem management and conservation endeavors.

#### *4.6. Limitation and Future Direction*

This study provides an objective analysis of China's terrestrial ecosystem carbon sink capacity over the past four decades, examining spatial-scale variations and nonlinear development trends. It also investigates the influence of land use patterns, temperature, and precipitation on the spatiotemporal evolution of this capacity. However, landscape indices calculations rely on the accuracy and resolution of remote sensing data. Lower data quality or an insufficient resolution may adversely affect the reliability and accuracy of these indices. In EEMD, certain parameter selections require subjective judgment and empirical consideration, such as those pertaining to noise standard deviation and decomposition scales. However, these parameter choices may influence the final outcomes. Meanwhile, this research focuses solely on hydrothermal factors when studying the impact of meteorological factors on the carbon sink pattern in Xinjiang. Furthermore, the study fails to investigate the strength of the correlation between landscape patterns and a range of climate-related and natural factors. Thus, it becomes imperative not only to evaluate different landscape indicators to determine the most suitable ones but also to account for the influence of various factors on NEP in future research. Additionally, the carbon sink capacity of terrestrial ecosystems is affected by diverse natural factors, including solar radiation, CO<sub>2</sub> concentration, and nitrogen deposition [99]. Hence, in future research, it is essential to consider coupling multiple factors, comprehensively analyze the impacts of various influencing factors on changes in terrestrial ecosystem carbon sink capacity, and provide theoretical support for decision makers to formulate short-term and long-term ecological carbon sequestration and regulation goals.

## 5. Conclusions

This study employs the EEMD trend method to examine the nonlinear variations in NEP in the Xinjiang region and further assesses the impact of climatic changes on the carbon sequestration capability of Xinjiang terrestrial ecosystems by correlating the detrended NEP data from EEMD with meteorological factors. The primary conclusions drawn are as follows:

The NEP changes in the Xinjiang region primarily follow a 3-year cycle, with an average variance contribution rate of 42.8%, showcasing a short-term fluctuating growth trend. Additionally, the 5-year cyclical changes significantly contribute to NEP variations (29.7%). The areas mainly affected by these short-term fluctuations are predominantly located on the northern slopes of the Tianshan Mountains, which are characterized by alpine meadows, grasslands, and wetland vegetation. Meanwhile, the 7-year scale has an average variance contribution rate of over 10% and areas primarily impacted include the northern parts of Altay and Tacheng, as well as Yili, Bortala, and Hejing County in Bazhou. These areas feature a mix of coniferous forests, mountain shrubs, and farmlands, thus making them susceptible to long-term interannual variations.

A significant portion of the study area (53.32%) displays no notable NEP variation trend. These areas are predominantly located in the northern region and characterized by alpine meadow grasslands and temperate grasslands. For areas with significant NEP changes, they mainly center on the Tianshan northern slope urban agglomeration, which is dominated by coniferous belts, meadow grasslands, mountain shrubs, and wetlands. The trend here primarily follows an initial decrease followed by an increase, accounting for about 35% of the overall change. The areas where the NEP shows a continuous decrease or an initial increase followed by a decrease occupy almost 7% of the region, suggesting a potential risk for NEP decline in the remaining parts.

The landscape pattern in the Xinjiang region of China has undergone significant changes, exhibiting trends towards increased dispersion, complexity, diversity, and uniformity. This study reveals that the PD, AWMPFD, SHDI, and MSIEI predominantly show an increasing trend, while the LPI and CONTAG primarily exhibit a decreasing trend. This suggests a general rise in patch fragmentation and shape intricacy, coupled with improved diversity and consistency in land use categories.

However, land use patterns also influence the changes in NEP. For instance, urbanization may lead to a carbon source shift in some areas, whereas afforestation contributes to an increase in carbon sequestration. This study reveals a positive correlation between LPI or MSIEI and NEP, indicating that an expansion in dominant patch area and a balanced distribution of patches contribute to an increase in NEP. On the other hand, CONTAG, as well as AWMPFD, SHDI, and PD, exhibit a significant negative correlation with NEP. This indicates that high land use type aggregation, shape complexity, diversity, and fragmentation inhibit increases in NEP.

In Xinjiang, the spatial correlation between NEP and climatic factors is evident, with approximately 62% of the area demonstrating a positive correlation with temperature. Within this region, 33% exhibits a significant positive correlation, notably across the Tianshan Mountains and the Kunlun Mountains, while 38% shows a negative correlation, with 22% displaying a significant negative trend, primarily in plains and deserts. Nearly 95% of the areas show a positive spatial correlation between NEP and precipitation, with 83% being statistically significant, while only 5% has a negative relationship. Moreover, the NEP changes in Xinjiang are more sensitive to precipitation changes and the increasing precipitation levels positively contribute to the region's NEP augmentation.

**Author Contributions:** Conceptualization, Y.Z. and J.Z. (Jianghua Zheng); methodology, Y.Z. and W.H.; writing—original draft preparation, Y.Z.; writing—review and editing, J.Z. (Jianghua Zheng), W.H. and L.L.; visualization, W.H. and L.L.; supervision, J.Z. (Jianghua Zheng); project administration, J.Z. (Jianghua Zheng), C.M. and J.Z. (Jianli Zhang); funding acquisition, J.Z. (Jianghua Zheng), C.M. and J.Z. (Jianli Zhang). All authors have read and agreed to the published version of the manuscript.

**Funding:** This research was supported by the project of “Impact of Extreme Drought on Grassland Net Primary Productivity in Xinjiang” (202105140044) by the Grassland Station of Xinjiang Uygur Autonomous Region.

**Institutional Review Board Statement:** Not applicable.

**Informed Consent Statement:** Not applicable.

**Data Availability Statement:** The data that support the findings of this study are available from the corresponding authors upon reasonable request.

**Acknowledgments:** We are thankful for the data support provided by the Grassland Station of Xinjiang Uygur Autonomous Region and all the authors for their contributions. The authors sincerely thank the anonymous reviewers who made valuable comments on this paper.

**Conflicts of Interest:** The authors declare no conflict of interest.

## References

- Jiao, K.; Liu, Z.; Wang, W.; Yu, K.; McGrath, M.; Xu, W. Carbon cycle responses to climate change across China’s terrestrial ecosystem: Sensitivity and driving process. *Sci. Total Environ.* **2024**, *915*, 170053. [\[CrossRef\]](#)
- Friedlingstein, P.; O’Sullivan, M.; Jones, M.W.; Andrew, R.M.; Hauck, J.; Olsen, A.; Peters, G.P.; Peters, W.; Pongratz, J.; Sitch, S.; et al. Global Carbon Budget 2020. *Earth. Syst. Sci. Data.* **2020**, *12*, 3269–3340. [\[CrossRef\]](#)
- Yu, G.R.; Zhu, X.J.; Fu, Y.L.; He, H.L.; Wang, Q.F.; Wen, X.F.; Li, X.R.; Zhang, L.M.; Zhang, L.; Su, W.; et al. Spatial patterns and climate drivers of carbon fluxes in terrestrial ecosystems of China. *Glob. Chang. Biol.* **2013**, *19*, 798–810. [\[CrossRef\]](#) [\[PubMed\]](#)
- Fernández-Martínez, M.; Vicca, S.; Janssens, I.A.; Sardans, J.; Luyssaert, S.; Campioli, M.; Chapin Iii, F.S.; Ciais, P.; Malhi, Y.; Obersteiner, M.; et al. Nutrient availability as the key regulator of global forest carbon balance. *Nat. Clim. Chang.* **2014**, *4*, 471–476. [\[CrossRef\]](#)
- Barnes, D.K.A.; Sands, C.J.; Paulsen, M.L.; Moreno, B.; Moreau, C.; Held, C.; Downey, R.; Bax, N.; Stark, J.S.; Zwierschke, N. Societal importance of Antarctic negative feedbacks on climate change: Blue carbon gains from sea ice, ice shelf and glacier losses. *Sci. Nat.* **2021**, *108*, 43. [\[CrossRef\]](#) [\[PubMed\]](#)
- Gaur, S.; Mittal, A.; Bandyopadhyay, A.; Holman, I.; Singh, R. Spatio-temporal analysis of land use and land cover change: A systematic model inter-comparison driven by integrated modelling techniques. *Int. J. Remote Sens.* **2020**, *41*, 9229–9255. [\[CrossRef\]](#)
- Xue, S.; Ma, B.; Wang, C.; Li, Z. Identifying key landscape pattern indices influencing the NPP: A case study of the upper and middle reaches of the Yellow River. *Ecol. Modell.* **2023**, *484*, 110457. [\[CrossRef\]](#)
- Xu, X.; Yang, G.; Tan, Y.; Tang, X.; Jiang, H.; Sun, X.; Zhuang, Q.; Li, H. Impacts of land use changes on net ecosystem production in the Taihu Lake Basin of China from 1985 to 2010. *J. Geophys. Res.-Biogeosci.* **2017**, *122*, 690–707. [\[CrossRef\]](#)
- Gao, Z.; Liu, J.; Cao, M.; Li, K.; Tao, B. Impacts of land-use and climate changes on ecosystem productivity and carbon cycle in the cropping-grazing transitional zone in China. *Sci. China Ser. D Earth Sci.* **2005**, *48*, 1479–1491. [\[CrossRef\]](#)
- Tang, Z.; Wang, Y.; Fu, M.; Xue, J. The role of land use landscape patterns in the carbon emission reduction: Empirical evidence from China. *Ecol. Indic.* **2023**, *156*, 111176. [\[CrossRef\]](#)
- Yang, H.; Hu, D.; Peng, F.; Wang, Y. Exploring the Response of Net Primary Productivity Variations to Land Use/Land Cover Change: A Case Study in Anhui, China. *Pol. J. Environ. Stud.* **2019**, *28*, 3971–3984. [\[CrossRef\]](#)
- Bai, Y.; Deng, X.; Weng, C.; Hu, Y.; Zhang, S.; Wang, Y. Investigating climate adaptation in semi-arid pastoral social-ecological system: A case in Hulun Buir, China. *Environ. Sustain. Indic.* **2024**, *21*, 100321. [\[CrossRef\]](#)
- Xu, M.; Wen, X.; Wang, H.; Zhang, W.; Dai, X.; Song, J.; Wang, Y.; Fu, X.; Liu, Y.; Sun, X.; et al. Effects of climatic factors and ecosystem responses on the inter-annual variability of evapotranspiration in a coniferous plantation in subtropical China. *PLoS ONE* **2014**, *9*, 85593. [\[CrossRef\]](#)
- Chapin, F.S.; Woodwell, G.M.; Randerson, J.T.; Rastetter, E.B.; Lovett, G.M.; Baldocchi, D.D.; Clark, D.A.; Harmon, M.E.; Schimel, D.S.; Valentini, R.; et al. Reconciling Carbon-cycle Concepts, Terminology, and Methods. *Ecosystems* **2006**, *9*, 1041–1050. [\[CrossRef\]](#)
- Pan, J.; Dong, L. Spatio-temporal variation in vegetation net primary productivity and its relationship with climatic factors in the Shule River basin from 2001 to 2010. *Hum. Ecol. Risk Assess.* **2017**, *24*, 797–818. [\[CrossRef\]](#)
- Zhang, T.; Zhang, Y.; Xu, M.; Xi, Y.; Zhu, J.; Zhang, X.; Wang, Y.; Li, Y.; Shi, P.; Yu, G.; et al. Ecosystem response more than climate variability drives the inter-annual variability of carbon fluxes in three Chinese grasslands. *Agric. Forest. Meteorol.* **2016**, *225*, 48–56. [\[CrossRef\]](#)
- Wang, Y.-R.; Buchmann, N.; Hessen, D.O.; Stordal, F.; Erisman, J.W.; Vollsnes, A.V.; Andersen, T.; Dolman, H. Disentangling effects of natural and anthropogenic drivers on forest net ecosystem production. *Sci. Total Environ.* **2022**, *839*, 156326. [\[CrossRef\]](#) [\[PubMed\]](#)
- Huang, C.; Sun, C.; Nguyen, M.; Wu, Q.; He, C.; Yang, H.; Tu, P.; Hong, S. Spatio-temporal dynamics of terrestrial Net ecosystem productivity in the ASEAN from 2001 to 2020 based on remote sensing and improved CASA model. *Ecol. Indic.* **2023**, *154*, 110920. [\[CrossRef\]](#)

19. Liu, H.; Xu, X.; Lin, Z.; Zhang, M.; Mi, Y.; Huang, C.; Yang, H. Climatic and human impacts on quasi-periodic and abrupt changes of sedimentation rate at multiple time scales in Lake Taihu, China. *J. Hydrol.* **2016**, *543*, 739–748. [[CrossRef](#)]
20. Shi, P.; Li, N.; Ye, Q.; Dong, W.; Han, G.; Fang, W. Research on integrated disaster risk governance in the context of global environmental change. *Int. J. Disaster Risk Sci.* **2010**, *1*, 17–23. [[CrossRef](#)]
21. Liu, J.; Wang, Z.; Duan, Y.; Li, X.; Zhang, M.; Liu, H.; Xue, P.; Gong, H.; Wang, X.; Chen, Y.; et al. Effects of land use patterns on the interannual variations of carbon sinks of terrestrial ecosystems in China. *Ecol. Indic.* **2023**, *146*, 109914. [[CrossRef](#)]
22. Liu, H.; Jia, J.; Lin, Z.; Wang, Z.; Gong, H. Relationship between net primary production and climate change in different vegetation zones based on EEMD detrending—A case study of Northwest China. *Ecol. Indic.* **2021**, *122*, 107276. [[CrossRef](#)]
23. Pan, N.; Feng, X.; Fu, B.; Wang, S.; Ji, F.; Pan, S. Increasing global vegetation browning hidden in overall vegetation greening: Insights from time-varying trends. *Remote Sens. Environ.* **2018**, *214*, 59–72. [[CrossRef](#)]
24. Wang, Z.; Zhong, J.; Lan, H.; Wang, Z.; Sha, Z. Association analysis between spatiotemporal variation of net primary productivity and its driving factors in inner Mongolia, China during 1994–2013. *Ecol. Indic.* **2019**, *105*, 355–364. [[CrossRef](#)]
25. Zhang, L.; Ren, X.; Wang, J.; He, H.; Wang, S.; Wang, M.; Piao, S.; Yan, H.; Ju, W.; Gu, F.; et al. Interannual variability of terrestrial net ecosystem productivity over China: Regional contributions and climate attribution. *Environ. Res. Lett.* **2019**, *14*, 014003. [[CrossRef](#)]
26. Liu, Y.; Zhao, W.; Hua, T.; Wang, S.; Fu, B. Slower vegetation greening faced faster social development on the landscape of the Belt and Road region. *Sci. Total Environ.* **2019**, *697*, 134103. [[CrossRef](#)]
27. Li, Y.; Yao, N.; Chau, H.W. Influences of removing linear and nonlinear trends from climatic variables on temporal variations of annual reference crop evapotranspiration in Xinjiang, China. *Sci. Total Environ.* **2017**, *592*, 680–692. [[CrossRef](#)]
28. De Beurs, K.M.; Henebry, G.M. A statistical framework for the analysis of long image time series. *Int. J. Remote Sens.* **2007**, *26*, 1551–1573. [[CrossRef](#)]
29. Wu, Z.; Huang, N.E.; Long, S.R.; Peng, C.-K. On the trend, detrending, and variability of nonlinear and nonstationary time series. *Proc. Natl. Acad. Sci. USA* **2007**, *104*, 14889–14894. [[CrossRef](#)]
30. Franzke, C. Multi-scale analysis of teleconnection indices: Climate noise and nonlinear trend analysis. *Nonlinear Process. Geophys.* **2009**, *16*, 65. [[CrossRef](#)]
31. Xia, N.; Hai, W.; Tang, M.; Song, J.; Quan, W.; Zhang, B.; Ma, Y. Spatiotemporal evolution law and driving mechanism of production–living–ecological space from 2000 to 2020 in Xinjiang, China. *Ecol. Indic.* **2023**, *154*, 110807. [[CrossRef](#)]
32. Liu, Y.; Yuan, X.; Li, J.; Qian, K.; Yan, W.; Yang, X.; Ma, X. Trade-offs and synergistic relationships of ecosystem services under land use change in Xinjiang from 1990 to 2020: A Bayesian network analysis. *Sci. Total Environ.* **2023**, *858*, 160015. [[CrossRef](#)]
33. Lian, X.; Jiao, L.; Hu, Y.; Liu, Z. Future climate imposes pressure on vulnerable ecological regions in China. *Sci. Total Environ.* **2023**, *858*, 159995. [[CrossRef](#)]
34. Yan, M.; Sun, H.; Gu, K. Driving factors and key emission reduction paths of Xinjiang industries carbon emissions: An industry chain perspective. *J. Clean. Prod.* **2022**, *374*, 133879. [[CrossRef](#)]
35. Mamtimin, B.; Et-Tantawi, A.M.M.; Schaefer, D.; Meixner, F.X.; Domroes, M. Recent trends of temperature change under hot and cold desert climates: Comparing the Sahara (Libya) and Central Asia (Xinjiang, China). *J. Arid. Environ.* **2011**, *75*, 1105–1113. [[CrossRef](#)]
36. Li, C.; Zhang, C.; Luo, G.; Chen, X. Modeling the carbon dynamics of the dryland ecosystems in Xinjiang, China from 1981 to 2007—The spatiotemporal patterns and climate controls. *Ecol. Modell.* **2013**, *267*, 148–157. [[CrossRef](#)]
37. Wu, Z.; Zhang, H.; Krause, C.M.; Cobb, N.S. Climate change and human activities: A case study in Xinjiang, China. *Clim. Chang.* **2010**, *99*, 457–472. [[CrossRef](#)]
38. Chen, J.M.; Ju, W.; Ciaiss, P.; Viovy, N.; Liu, R.; Liu, Y.; Lu, X. Vegetation structural change since 1981 significantly enhanced the terrestrial carbon sink. *Nat. Commun.* **2019**, *10*, 4259. [[CrossRef](#)] [[PubMed](#)]
39. Muñoz Sabater, J. ERA5-Land Monthly Averaged Data from 1950 to Present. Copernicus Climate Change Service (C3S) Climate Data Store (CDS). Available online: <https://doi.org/10.24381/cds.68d2bb30> (accessed on 16 September 2023).
40. Peng, S. High-Spatial-Resolution Monthly Precipitation Dataset over China during 1901–2017. *Earth Syst. Sci. Data* **2019**, *11*, 193–1946. [[CrossRef](#)]
41. Yang, H.; Zhong, X.; Deng, S.; Xu, H. Assessment of the impact of LUCC on NPP and its influencing factors in the Yangtze River basin, China. *Catena* **2021**, *206*, 105543. [[CrossRef](#)]
42. Liu, J.; Kuang, W.; Zhang, Z.; Xu, X.; Qin, Y.; Ning, J.; Zhou, W.; Zhang, S.; Li, R.; Yan, C.; et al. Spatiotemporal characteristics, patterns, and causes of land-use changes in China since the late 1980s. *J. Geogr. Sci.* **2014**, *24*, 195–210. [[CrossRef](#)]
43. Liu, H.; Zhang, M.; Lin, Z.; Xu, X. Spatial heterogeneity of the relationship between vegetation dynamics and climate change and their driving forces at multiple time scales in Southwest China. *Agric. Forest. Meteorol.* **2018**, *256–257*, 10–21. [[CrossRef](#)]
44. Liu, H.; Zhang, M.; Lin, Z. Relative importance of climate changes at different time scales on net primary productivity a case study of the Karst area of northwest Guangxi, China. *Environ. Monit. Assess.* **2017**, *189*, 539. [[CrossRef](#)]
45. Ji, F.; Wu, Z.; Huang, J.; Chassignet, E.P. Evolution of land surface air temperature trend. *Nat. Clim. Chang.* **2014**, *4*, 462–466. [[CrossRef](#)]
46. Wu, Z.; Huang, N.E. Ensemble empirical mode decomposition: A noiseassisted data analysis method. *Adv. Adapt. Data Anal.* **2009**, *1*, 1–41. [[CrossRef](#)]

47. Huang, N.E.; Wu, Z. A review on Hilbert-Huang transform: Method and its applications to geophysical studies. *Rev. Geophys.* **2008**, *46*, RG2006–RG2008. [[CrossRef](#)]
48. Wu, Z.; Huang, N.E.; Wallace, J.M.; Smoliak, B.V.; Chen, X. On the time-varying trend in global-mean surface temperature. *Clim. Dynam.* **2011**, *37*, 759–773. [[CrossRef](#)]
49. Hawinkel, P.; Swinnen, E.; Lhermitte, S.; Verbist, B.; Van Orshoven, J.; Muys, B. A time series processing tool to extract climate-driven interannual vegetation dynamics using Ensemble Empirical Mode Decomposition (EEMD). *Remote Sens. Environ.* **2015**, *169*, 375–389. [[CrossRef](#)]
50. Zhao, Y.; Zheng, R.; Zheng, F.; Zhong, K.; Fu, J.; Zhang, J.; Flanagan, D.C.; Xu, X.; Li, Z. Spatiotemporal distribution of agrometeorological disasters in China and its impact on grain yield under climate change. *Int. J. Disaster Risk Reduct.* **2023**, *95*, 103823. [[CrossRef](#)]
51. Zhang, M.; Li, W.; Zhang, L.; Jin, H.; Mu, Y.; Wang, L. A Pearson correlation-based adaptive variable grouping method for large-scale multi-objective optimization. *Inf. Sci.* **2023**, *639*, 118737. [[CrossRef](#)]
52. Lin, Y.; Wiegand, K. Low  $R^2$  in ecology: Bitter, or B-side? *Ecol. Indic.* **2023**, *153*, 110406. [[CrossRef](#)]
53. Su, N.; Jarvie, S.; Yan, Y.; Gong, X.; Li, F.; Han, P.; Zhang, Q. Landscape context determines soil fungal diversity in a fragmented habitat. *Catena* **2022**, *213*, 106163. [[CrossRef](#)]
54. Zhou, Y.; Yue, D.; Guo, J.; Chen, G.; Wang, D. Spatial correlations between landscape patterns and net primary productivity: A case study of the Shule River Basin, China. *Ecol. Indic.* **2021**, *130*, 108067. [[CrossRef](#)]
55. Yang, H.; Zhong, X.; Deng, S.; Nie, S. Impact of LUCC on landscape pattern in the Yangtze River Basin during 2001–2019. *Ecol. Inform.* **2022**, *69*, 101631. [[CrossRef](#)]
56. Du, J.; Shu, J.; Yin, J.; Yuan, X.; Jiaerheng, A.; Xiong, S.; He, P.; Liu, W. Analysis on spatio-temporal trends and drivers in vegetation growth during recent decades in Xinjiang, China. *Int. J. Appl. Earth. Obs.* **2015**, *38*, 216–228. [[CrossRef](#)]
57. Xu, D.; Mou, W.; Wang, X.; Zhang, R.; Gao, T.; Ai, D.; Yuan, J.; Zhang, R.; Fang, X. Consistent responses of ecosystem  $CO_2$  exchange to grassland degradation in alpine meadow of the Qinghai-Tibetan Plateau. *Ecol. Indic.* **2022**, *141*, 109036. [[CrossRef](#)]
58. Gong, H.; Cheng, Q.; Jin, H.; Ren, Y. Effects of temporal, spatial, and elevational variation in bioclimatic indices on the NDVI of different vegetation types in Southwest China. *Ecol. Indic.* **2023**, *154*, 110499. [[CrossRef](#)]
59. Jiang, L.; Liu, W.; Liu, B.; Yuan, Y.; Bao, A. Monitoring vegetation sensitivity to drought events in China. *Sci. Total Environ.* **2023**, *893*, 164917. [[CrossRef](#)]
60. Jiapaer, G.; Liang, S.; Yi, Q.; Liu, J. Vegetation dynamics and responses to recent climate change in Xinjiang using leaf area index as an indicator. *Ecol. Indic.* **2015**, *58*, 64–76. [[CrossRef](#)]
61. Chen, Y.; Li, Y.; Duan, Y.; Wang, L.; Wang, X.; Yao, C.; Chen, Y.; Cao, W.; Niu, Y. Patterns and driving factors of soil ecological stoichiometry in typical ecologically fragile areas of China. *Catena* **2022**, *219*, 106628. [[CrossRef](#)]
62. Lou, H.; Yang, S.; Shi, X.; Zhang, J.; Pan, Z.; Li, C.; Zhang, Y.; Zhou, B.; Li, H.; Shi, Y.; et al. Whether the enhanced terrestrial vegetation carbon sink affect the water resources in the middle-low latitude karst areas of China? *J. Hydrol.* **2023**, *620*, 129510. [[CrossRef](#)]
63. Shi, Z.; Xiang, F.; Guo, Y. Ecological risk of geohazards and its combination patterns: A case study of an ecologically fragile region, NW China. *Ecol. Inform.* **2023**, *77*, 102153. [[CrossRef](#)]
64. Luo, N.; Mao, D.; Wen, B.; Liu, X. Climate Change Affected Vegetation Dynamics in the Northern Xinjiang of China: Evaluation by SPEI and NDVI. *Land* **2020**, *9*, 90. [[CrossRef](#)]
65. Zhao, J.; Ma, J.; Zhu, Y. Evaluating impacts of climate change on net ecosystem productivity (NEP) of global different forest types based on an individual tree-based model FORCCHN and remote sensing. *Global. Planet. Chang.* **2019**, *182*, 103010. [[CrossRef](#)]
66. Cao, X.; Chen, X.; Bao, A.; Wang, Q. Response of vegetation to temperature and precipitation in Xinjiang during the period of 1998–2009. *J. Arid Land* **2011**, *3*, 94–103. [[CrossRef](#)]
67. Yin, J.; Wang, D.; Li, H. Spatial optimization of rural settlements in ecologically fragile regions: Insights from a social-ecological system. *Habitat Int.* **2023**, *138*, 102854. [[CrossRef](#)]
68. Liu, X.; Ma, J.; Ma, Z.-W.; Li, L.-H. Soil nutrient contents and stoichiometry as affected by land-use in an agro-pastoral region of northwest China. *Catena* **2017**, *150*, 146–153. [[CrossRef](#)]
69. Chen, C.; Park, T.; Wang, X.; Piao, S.; Xu, B.; Chaturvedi, R.K.; Fuchs, R.; Brovkin, V.; Ciais, P.; Fensholt, R.; et al. China and India lead in greening of the world through land-use management. *Nat. Sustain.* **2019**, *2*, 122–129. [[CrossRef](#)]
70. Sun, S.; Ouyang, S.; Hu, Y.; Zhao, Z.; Liu, M.; Chen, L.; Zeng, Y.; Peng, C.; Zhou, X.; Xiang, W. rTRIPLEXCWFlux: An R package for carbon–water coupling model to simulate net ecosystem productivity and evapotranspiration in forests. *Environ. Modell. Softw.* **2023**, *162*, 105661. [[CrossRef](#)]
71. Chen, T.; Tang, G.; Yuan, Y.; Guo, H.; Xu, Z.; Jiang, G.; Chen, X. Unraveling the relative impacts of climate change and human activities on grassland productivity in Central Asia over last three decades. *Sci. Total Environ.* **2020**, *743*, 140649. [[CrossRef](#)]
72. Aizizi, Y.; Kasimu, A.; Liang, H.; Zhang, X.; Zhao, Y.; Wei, B. Evaluation of ecological space and ecological quality changes in urban agglomeration on the northern slope of the Tianshan Mountains. *Ecol. Indic.* **2023**, *146*, 109896. [[CrossRef](#)]
73. Yu, T.; Abulizi, A.; Xu, Z.; Jiang, J.; Akbar, A.; Ou, B.; Xu, F. Evolution of environmental quality and its response to human disturbances of the urban agglomeration in the northern slope of the Tianshan Mountains. *Ecol. Indic.* **2023**, *153*, 110481. [[CrossRef](#)]

74. Yibo, Y.; Ziyuan, C.; Xiaodong, Y.; Simayi, Z.; Shengtian, Y. The temporal and spatial changes of the ecological environment quality of the urban agglomeration on the northern slope of Tianshan Mountain and the influencing factors. *Ecol. Indic.* **2021**, *133*, 108380. [[CrossRef](#)]
75. Yue, Z.; Liu, H.; Xu, Z.; Wang, Y. Evaluation of sustainability in northern Xinjiang based on ecological footprint-planetary boundary system framework. *Ecol. Indic.* **2023**, *150*, 110270. [[CrossRef](#)]
76. Yang, H.; Mu, S.; Li, J. Effects of ecological restoration projects on land use and land cover change and its influences on territorial NPP in Xinjiang, China. *Catena* **2014**, *115*, 85–95. [[CrossRef](#)]
77. Han, C.; Zheng, J.; Guan, J.; Yu, D.; Lu, B. Evaluating and simulating resource and environmental carrying capacity in arid and semiarid regions: A case study of Xinjiang, China. *J. Clean. Prod.* **2022**, *338*, 130646. [[CrossRef](#)]
78. Chen, C.; Zhao, G.; Zhang, Y.; Bai, Y.; Tian, P.; Mu, X.; Tian, X. Linkages between soil erosion and long-term changes of landscape pattern in a small watershed on the Chinese Loess Plateau. *Catena* **2023**, *220*, 106659. [[CrossRef](#)]
79. Yu, J.; Long, A.; Lai, X.; Elbeltagi, A.; Deng, X.; Gu, X.; Heng, T.; Cheng, H.; van Oel, P. Evaluating sustainable intensification levels of dryland agriculture: A focus on Xinjiang, China. *Ecol. Indic.* **2024**, *158*, 111448. [[CrossRef](#)]
80. Li, X.; Dong, W.; Liu, Y.; Yang, Y. Tracking the urban expansion and its driving mechanisms behind Xinjiang Production and Construction Corps (XPCC): Evidence from morphology and landscapes. *Habitat Int.* **2022**, *126*, 102599. [[CrossRef](#)]
81. Li, X.; Zheng, Z.; Shi, D.; Han, X.; Zhao, M. New urbanization and carbon emissions intensity reduction: Mechanisms and spatial spillover effects. *Sci. Total Environ.* **2023**, *905*, 167172. [[CrossRef](#)]
82. Han, L.; Wang, Z.; Wei, M.; Wang, M.; Shi, H.; Ruckstuhl, K.; Yang, W.; Alves, J. Small patches play a critical role in the connectivity of the Western Tianshan landscape, Xinjiang, China. *Ecol. Indic.* **2022**, *144*, 109542. [[CrossRef](#)]
83. Zhang, F.; Li, M.; Zhang, S.; Liu, J.; Ren, Y.; Cao, Y.; Li, F. China's National Reserve Forest Project contribution to carbon neutrality and path to profitability. *For. Policy Econ.* **2024**, *160*, 103146. [[CrossRef](#)]
84. Cai, Y.; Zhang, F.; Duan, P.; Yung Jim, C.; Weng Chan, N.; Shi, J.; Liu, C.; Wang, J.; Bahtebay, J.; Ma, X. Vegetation cover changes in China induced by ecological restoration-protection projects and land-use changes from 2000 to 2020. *Catena* **2022**, *217*, 106530. [[CrossRef](#)]
85. Guo, L.; Liu, R.; Shoaib, M.; Men, C.; Wang, Q.; Miao, Y.; Jiao, L.; Wang, Y.; Zhang, Y. Impacts of landscape change on net primary productivity by integrating remote sensing data and ecosystem model in a rapidly urbanizing region in China. *J. Clean. Prod.* **2021**, *325*, 129314. [[CrossRef](#)]
86. Wei, B.; Kasimu, A.; Reheman, R.; Zhang, X.; Zhao, Y.; Aizizi, Y.; Liang, H. Spatiotemporal characteristics and prediction of carbon emissions/absorption from land use change in the urban agglomeration on the northern slope of the Tianshan Mountains. *Ecol. Indic.* **2023**, *151*, 110329. [[CrossRef](#)]
87. Zeng, J.; Zhou, T.; Wang, Q.; Xu, Y.; Lin, Q.; Zhang, Y.; Wu, X.; Zhang, J.; Liu, X. Spatial patterns of China's carbon sinks estimated from the fusion of remote sensing and field-observed net primary productivity and heterotrophic respiration. *Ecol. Inform.* **2023**, *76*, 102752. [[CrossRef](#)]
88. Wang, D.-D.; Shi, X.-Z.; Wang, H.-J.; Weindorf, D.C.; Yu, D.-S.; Sun, W.-X.; Ren, H.-Y.; Zhao, Y.-C. Scale effect of climate on soil organic carbon in the Uplands of Northeast China. *J. Soils Sediments* **2009**, *10*, 1007–1017. [[CrossRef](#)]
89. Yang, Y.; Fang, J.; Ma, W.; Smith, P.; Mohammad, A.; Wang, S.; Wang, W.E.I. Soil carbon stock and its changes in northern China's grasslands from 1980s to 2000s. *Glob. Chang. Biol.* **2010**, *16*, 3036–3047. [[CrossRef](#)]
90. Xue, Y.; Bai, X.; Zhao, C.; Tan, Q.; Li, Y.; Luo, G.; Wu, L.; Chen, F.; Li, C.; Ran, C.; et al. Spring photosynthetic phenology of Chinese vegetation in response to climate change and its impact on net primary productivity. *Agric. Forest. Meteorol.* **2023**, *342*, 109734. [[CrossRef](#)]
91. Liu, Z.; Zhou, Q.; Ma, Q.; Kuang, W.; Daryanto, S.; Wang, L.; Wu, J.; Liu, B.; Zhu, J.; Cao, C.; et al. Scale effect of climate factors on soil organic carbon stock in natural grasslands of northern China. *Ecol. Indic.* **2023**, *146*, 109757. [[CrossRef](#)]
92. Wang, Q.; Zhai, P.-M.; Qin, D.-H. New perspectives on 'warming-wetting' trend in Xinjiang, China. *Adv. Clim. Chang. Res.* **2020**, *11*, 252–260. [[CrossRef](#)]
93. Naem, M.; Shahzad, K.; Saqib, S.; Shahzad, A.; Nasrullah; Younas, M.; Afridi, M.I. The *Solanum melongena* COP1LIKE manipulates fruit ripening and flowering time in tomato (*Solanum lycopersicum*). *Plant Growth Regul.* **2022**, *96*, 369–382. [[CrossRef](#)]
94. Naem, M.; Waseem, M.; Zhu, Z.; Zhang, L. Downregulation of SIGRAS15 manipulates plant architecture in tomato (*Solanum lycopersicum*). *Dev. Genes Evol.* **2020**, *230*, 1–12. [[CrossRef](#)]
95. Liu, L.; Zheng, J.; Guan, J.; Han, W.; Liu, Y. Grassland cover dynamics and their relationship with climatic factors in China from 1982 to 2021. *Sci. Total Environ.* **2023**, *905*, 167067. [[CrossRef](#)]
96. Zhang, R.; Guo, J.; Liang, T.; Feng, Q. Grassland vegetation phenological variations and responses to climate change in the Xinjiang region, China. *Quat. Int.* **2019**, *513*, 56–65. [[CrossRef](#)]
97. Yu, T.; Jiapaer, G.; Long, G.; Li, X.; Jing, J.; Liu, Y.; De Maeyer, P.; Van de Voorde, T. Interannual and seasonal relationships between photosynthesis and summer soil moisture in the Ili River basin, Xinjiang, 2000–2018. *Sci. Total Environ.* **2023**, *856*, 159191. [[CrossRef](#)] [[PubMed](#)]



98. Zhang, X.; Chen, Y.; Zhang, Q.; Xia, Z.; Hao, H.; Xia, Q. Potential evapotranspiration determines changes in the carbon sequestration capacity of forest and grass ecosystems in Xinjiang, Northwest China. *Glob. Ecol. Conserv.* **2023**, *48*, e02737. [[CrossRef](#)]
99. Tian, H.; Melillo, J.; Lu, C.; Kicklighter, D.; Liu, M.; Ren, W.; Xu, X.; Chen, G.; Zhang, C.; Pan, S.; et al. China's terrestrial carbon balance: Contributions from multiple global change factors. *Glob. Biogeochem. Cycles* **2011**, *25*, GB1007. [[CrossRef](#)]

**Disclaimer/Publisher's Note:** The statements, opinions and data contained in all publications are solely those of the individual author(s) and contributor(s) and not of MDPI and/or the editor(s). MDPI and/or the editor(s) disclaim responsibility for any injury to people or property resulting from any ideas, methods, instructions or products referred to in the content.